Development/Plasticity/Repair

Adenosine and Astrocytes Determine the Developmental Dynamics of Spike Timing-Dependent Plasticity in the Somatosensory Cortex

Irene Martínez-Gallego,[1] Mikel Pérez-Rodríguez,[1*] Heriberto Coatl-Cuaya,[1*] Gonzalo Flores,[2] and Antonio Rodríguez-Moreno[1]

[1]Laboratory of Cellular Neuroscience and Plasticity, Department of Physiology, Anatomy and Cell Biology, Universidad Pablo de Olavide, ES-41013 Seville, Spain, and [2]Instituto de Fisiología, Benemérita Universidad Autónoma de Puebla, Puebla CP 72570, México

During development, critical periods of synaptic plasticity facilitate the reordering and refinement of neural connections, allowing the definitive synaptic circuits responsible for correct adult physiology to be established. The L4–L2/3 synapses in the somatosensory cortex (S1) exhibit a presynaptic form of spike timing-dependent long-term depression (t-LTD) that probably fulfills a role in synaptic refinement. This t-LTD persists until the fourth postnatal week in mice, disappearing thereafter. When we investigated the mechanisms underlying this maturation-related loss of t-LTD in either sex mouse slices, we found that it could be completely recovered by antagonizing adenosine type 1 receptors. By contrast, an agonist of A_1R impeded the induction of t-LTD at P13–27. Furthermore, we found that the adenosine that mediated the loss of t-LTD at the end of the fourth week of development is most probably supplied by astrocytes. At more mature stages (P38–60), we found that the protocol used to induce t-LTD provokes t-LTP. We characterized the mechanisms underlying the induction of this form of LTP, and we found it to be expressed presynaptically, as witnessed by paired-pulse and coefficient of variation analysis. In addition, this form of presynaptic t-LTP requires the activation of NMDARs and mGlu1Rs, and the entry of Ca^{2+} into the postsynaptic neuron through L-type voltage-dependent Ca^{2+} channels. Nitric oxide is also required for t-LTP as a messenger in the postsynaptic neuron as are the adenosine and glutamate that are released in association with astrocyte signaling. These results provide direct evidence of the mechanisms that close the window of plasticity associated with t-LTD and that drive the switch in synaptic transmission from t-LTD to t-LTP at L4–L2/3 synapses, in which astrocytes play a central role.

Key words: adenosine; astrocyte; barrel cortex; critical period; glutamate; spike timing-dependent plasticity

Significance Statement

During development, critical periods of plasticity facilitate the reordering and refining of neural connections, allowing correct adult physiology to be established. The L4–L2/3 synapses in the somatosensory cortex exhibit a presynaptic form plasticity (LTD) that probably fulfills a role in synaptic refinement. It is present until the fourth postnatal week in mice, disappearing thereafter. The mechanisms that are responsible for this loss of plasticity are not clear. We describe here these mechanisms and those involved in the switch from LTD to LTP observed as the brain matures. Defining these events responsible for closing (and opening) plasticity windows may be important for brain repair, sensorial recovery, the treatment of neurodevelopmental disorders, and for educational policy.

Received Jan. 17, 2022; revised Apr. 18, 2022; accepted May 18, 2022.

Author contributions: A.R.-M. designed research; I.M-G., M.P.-R., and H.C.-C. performed research; G.F. analyzed data; A.R.-M. wrote the paper.

This work was supported by grants from the Spanish Agencia Estatal de Investigación/FEDER (Grant PID 2019-107677GB-I00) and the Junta de Andalucía/FEDER (Grant P20-00881), and Andalusian Government (Grants UPO-1258682 and P18-HO-4625) to A.R.-M. I.M.-G. was supported by a Formación de Profesorado Universitario PhD Fellowship from the Ministerio de Ciencia, Innovación y Universidades. M.P.-R. was supported by a PhD Fellowship from the Basque Regional Government. H.C.-C. was supported by a Consejo Nacional de Ciencia y Tecnología (Mexico) Fellowship for short-term visits. We thank Dr. Cristina Calvino for technical assistance, Prof. Philip Haydon and Dr. Joao Oliveira for sharing the dn-SNARE mice lines, and Dr. Mark Sefton for editorial assistance.

*M.P.-R. and H.C.-C. contributed equally to this work.

The authors declare no competing financial interests.

Correspondence should be addressed to Antonio Rodríguez-Moreno at arodmor@upo.es.

https://doi.org/10.1523/JNEUROSCI.0115-22.2022

Introduction

One of the most interesting properties of the mammalian brain is its ability to change in response to experience. This phenomenon, called plasticity (Ramón y Cajal, 1894), underlies the reorganization of cortical maps during development, as well as learning and memory processes in adults (Citri and Malenka, 2008; Bliss et al., 2014). Throughout development, activity and sensory-dependent plastic changes occur during permissive and critical periods, wherein environmental influences shape brain circuits and refine neural connections into the definitive adult circuits (Hensch, 2004, 2005). The closing of such permissive windows is associated with the loss of plasticity at particular

synapses, producing specific functional effects (Hensch, 2004). Long-term potentiation (LTP) and long-term depression (LTD) of synaptic transmission are the two best-known forms of plasticity. Spike timing-dependent plasticity (STDP) is a Hebbian form of synaptic plasticity detected in all species studied, from insects to humans, and it is a strong candidate to drive circuit remodeling during development, as well as learning and memory in adults (Debanne et al., 1994, 1998; Markram et al., 1997; Bi and Poo, 1998; Feldman, 2000, 2012). In STDP, the order and relative timing of presynaptic and postsynaptic action potentials (APs; spikes) determine the direction and magnitude of the synaptic changes. Thus, spike timing-dependent LTP (t-LTP) occurs when a presynaptic spike is followed by a postsynaptic spike, whereas spike timing-dependent LTD (t-LTD) is induced when this order is inverted, although some exceptions to this do exist (Feldman, 2012; Brzosko et al., 2019).

Presynaptic forms of t-LTD have been described in the visual and somatosensory cortices and in the hippocampus (Corlew et al., 2008; Rodríguez-Moreno et al., 2010; Brzosko et al., 2019). These forms of t-LTD are expressed presynaptically, and they disappear during the third to fifth weeks of postnatal development (Corlew et al., 2008; Rodríguez-Moreno et al., 2010; Andrade-Talavera et al., 2016; Bouvier et al., 2018; Brzosko et al., 2019; Pérez-Rodríguez et al., 2019). In the mouse barrel cortex, presynaptic t-LTD is lost by the fourth week of postnatal day (P) development (≈P25–42; Banerjee et al., 2009). This t-LTD is known to be dependent on postsynaptic Ca^{2+}, L-type voltage-dependent Ca^{2+} channels, mGlu5 receptor activation, phospholipase C, postsynaptic IP_3 receptor-mediated Ca^{2+} release from internal stores, postsynaptic endocannabinoid (eCB) synthesis, and activation of CB_1 receptors and astroglial signaling that delivers glutamate to NMDARs during its induction (Bender et al., 2006; Nevian and Sakmann, 2006; Brasier and Feldman, 2008; Rodríguez-Moreno and Paulsen, 2008; Min and Nevian, 2012; Rodríguez-Moreno et al., 2013; Banerjee et al., 2014). To date, it remains unclear what mechanisms are responsible for the loss of this plasticity during the fourth week of development (Banerjee et al., 2009). Moreover, it is unclear whether the closure of this window of plasticity is reversible or not and whether it is permanent, persisting throughout the lifetime of the animal. Defining the events responsible for closing plasticity windows is important when studying the brain responses to experience and injury. Indeed, defining such processes may have important implications for brain repair, sensorial recovery, the treatment of neurodevelopmental disorders, and even for educational policy.

Here, we studied the mechanisms driving the loss of t-LTD observed as L4–L2/3 synapses mature in the mouse barrel cortex using whole-cell patch-clamp recordings. As described previously, we found that t-LTD can be induced at L4–L2/3 synapses in young mice (P13–27) and that it is lost at the end of the fourth week of development (P28–37). We discovered that this developmental loss of t-LTD can be reversed by antagonizing adenosine type 1 receptors (A_1Rs) and, conversely, that the induction of t-LTD is impaired between P13 and P27 in the presence of an A_1R agonist. In addition, we found that the adenosine that mediates the loss of t-LTD at the end of the fourth week of development is released as a result of astrocyte signaling. We also explored what occurs after P37 at S1 L4–L2/3 synapses and, interestingly, we found that a post-before-pre protocol that induces t-LTD at P13–27 fails to induce plasticity at P28–37, although it does induce t-LTP at P38–60. Characterizing this form of t-LTP, the result of a switch from presynaptic t-LTD, paired-pulse ratio (PPR), and coefficient of variation (CV) analyses demonstrate its presynaptic nature. This t-LTP requires the activation of NMDARs and mGluR1, as well as a calcium flux through postsynaptic L-type calcium channels, calcium release from intracellular stores and signaling by nitric oxide (NO) as a retrograde messenger. The switch from presynaptic t-LTD to t-LTP is mediated by the activation of presynaptic A_1Rs by adenosine released as a result of astrocyte signaling. Finally, astrocytes seem to induce t-LTP not only by releasing adenosine but also by supplying glutamate. Thus, we reveal here the mechanisms underlying t-LTD loss during maturation and a developmental switch from presynaptic depression to presynaptic potentiation of synaptic transmission as the S1 matures, defining the mechanisms by which this form of t-LTP is induced.

Materials and Methods

Mice. All animal procedures were conducted in accordance with the European Union Directive 2010/63/EU regarding the protection of animals used for scientific purposes, and they were approved by the Ethics Committee of the Universidad Pablo de Olavide and the Ethics Committee of the Andalusian Government. C57BL/6 mice were obtained from Harlan Laboratories (Spain), and P13–60 mice of either sex were used. Animals were kept on a continuous 12 h light/dark cycle, at temperatures between 18 and 24°C, at 40–60% humidity, and with *ad libitum* access to food and water. In some experiments, dominant-negative (dn) SNARE mice (Pascual et al., 2005; Sardinha et al., 2017) of the same ages were used. These mice were not fed with doxycycline from birth, the supplement that drives transgene expression. In these mice, the human glial fibrillary acidic protein promoter mediates the expression of the tetracycline transactivator specifically in astrocytes, which in turn activates the tetracycline responsive element operator and drives the cytosolic expression of VAMP2/synaptobrevin II, as well as the enhanced green fluorescence protein. Expression of the dnSNARE transgene interferes with the formation of the SNARE complex, resulting in a blockade of exocytosis and impaired vesicular release in astrocytes (Sultan et al., 2015).

Slice preparation. Slices containing the barrel subfield of the somatosensory cortex were prepared as described previously (Agmon and Connors, 1991; Rodríguez-Moreno et al., 2013; Banerjee et al., 2014). Briefly, mice were anesthetized with isoflurane (2%) and decapitated, and their whole brain was removed and placed in an ice-cold solution containing the following (in mM, 300 $mOsm \cdot L^{-1}$): 126 NaCl, 3 KCl, 1.25 NaH_2PO_4, 2 $MgSO_4$, 2 $CaCl_2$, 26 $NaHCO_3$, and 10 glucose, pH 7.2. Slices (350 µm thick, Leica VT1000S Vibratome) were maintained oxygenated (95% O_2/5% CO_2) in the same solution for at least 1 h before use. Experiments were conducted at 30–34°C, during which the slices were superfused continuously with the solution indicated above.

Electrophysiological recordings. Slices containing the barrel cortex were identified and selected under a stereomicroscope. Two monopolar stimulation electrodes were placed at the base of a barrel (L4), and whole-cell patch-clamp recordings were obtained from L2/3 pyramidal cells located in the same barrel column with 5–7 MΩ borosilicate pipettes. The pipette solution contained the following (in mM, 290 $mOsm \cdot L^{-1}$): 110 potassium gluconate, 40 HEPES, 4 NaCl, 4 ATP-Mg, and 0.3 GTP, pH 7.2–7.3. Cells with a pyramidal-shaped soma were selected for recording using infrared, differential interference contrast optics. The neurons were verified as pyramidal cells through their characteristic regular spiking responses to positive current injection. Whole-cell recordings were obtained with an Axon MultiClamp 700B amplifier (Molecular Devices. Only cells with a stable resting membrane potential below −55 mV were assessed, and the cell recordings were excluded from the analysis if the series resistance changed by >15%. All recordings were low-pass filtered at 3 kHz and acquired at 10 kHz, and all the experiments were performed in current-clamp mode. To study plasticity, EPSPs were evoked alternately through two input pathways, test and control, each at 0.2 Hz. Stimulating electrodes were situated 200–400 µm from the cell soma, and the EPSPs were induced using brief current pulses (200 µs, 0.1–0.2 mA). Stimulation was adjusted to obtain an EPSP peak amplitude of ~3–5 mV in control conditions, and pathway independence was ensured by the lack of cross-facilitation when the pathways were

stimulated alternately at 50 ms intervals. Plasticity was assessed through the changes in the EPSP slope, measured in its rising phase as a linear fit between time points, corresponding to 25–30% and 70–75% of the peak amplitude under control conditions.

Plasticity protocols. After establishing a stable basal EPSP over 10 min, the test input was paired 100 times with a single postsynaptic spike. The single postsynaptic spike was evoked by a brief somatic current pulse (5 ms, 0.1–0.5 pA), whereas the control pathway was unstimulated during the pairing period. To induce t-LTD, the postsynaptic AP was evoked 18 ms before the onset of the EPSP. EPSP slopes were monitored for at least 30 min after the pairing protocol, and the presynaptic stimulation frequency remained constant throughout the experiment. Where appropriate, glutamate puffs were applied using a Picospritzer (Parker Hannifin). Glutamate was dissolved in the external solution and puffed through a micropipette over an astrocyte at a pressure of 10 psi for 50–200 ms, which did not affect patch clamping. For each experiment, 50–100 glutamate puffs were applied at 0.2 Hz after the recording neuron at baseline, 18 ms before the onset of the EPSP. EPSP slopes were monitored for 30 min after the protocol. In some experiments, different timings were used.

Pharmacology. The following compounds used here were purchased from Sigma-Aldrich: BAPTA (20 mM; catalog #A4926), N6-Cyclopentyladenosine (CPA; 60 nM; catalog #119135), and GDPβS (1 mM; catalog #G7637), as well as all the salts used to prepare the internal and external solutions. The following compounds were purchased from Tocris Bioscience: (+)−MK-801 maleate (500 μM; catalog #0924), D-AP5 (50 μM; catalog #0106), 8-cyclopentyl-1,3-dimethylxanthine (8-CPT; 2 μM; catalog #6137), cPTIO (100 μM; catalog #0772), L-glutamic acid (100 μM; catalog #0218), LY367385 (100 μM; catalog #1237), LY341495 (100 μM; catalog #1209), L-NAME (100 μM; catalog #0665), DETA NONOate (5 mM; catalog #6077), nimodipine (10 μM; catalog #0600), thapsigargin (10 μM; catalog #1138), bicuculline (10 μM; catalog #0130), and SCH50911 (20 μM; catalog #0984). These compounds were all dissolved in water except 8-CPT, nimodipine, and thapsigargin, which were dissolved in DMSO.

Data analysis. The data were analyzed with Clampfit 10.2 software (Molecular Devices), and the last 5 min of recording were used to estimate the changes in synaptic efficacy relative to the baseline. For the PPR experiments, two EPSPs were evoked for 30 s at the baseline frequency, at the beginning of the baseline recording (40 ms apart), and again 30 min after the end of the pairing protocol. The PPR was expressed as the slope of the second EPSP divided by the slope of the first EPSP. A CV analysis was conducted on the EPSP slopes (Rodríguez-Moreno and Paulsen, 2008).

The noise-free CV of the EPSP slopes was calculated as follows:

$$\mathrm{CV} = \sqrt{\sigma^2(\mathrm{EPSP}) - \sigma^2(\mathrm{noise})}/\mathrm{EPSP\ slope},$$

where $\sigma^2_{(\mathrm{EPSP})}$ and $\sigma^2_{(\mathrm{noise})}$ are the variance of the EPSP and baseline, respectively. The plot compares the variation in the mean EPSP slope (M) to the change in response variance of the EPSP slope ($1/\mathrm{CV}^2$). A comprehensive explanation can be found in Brock et al. (2020). Graphs were obtained using SigmaPlot 11.0.

Statistical analysis. For any comparisons between two groups a Mann–Whitney *U* test or Wilcoxon signed-rank test was used, as appropriate. For multiple comparisons to the same control, a Kruskal–Wallis test was used. The data are expressed as mean ± SEM, and p values <0.05 were considered significant, $^*p < 0.05$, $^{**}p < 0.01$, $^{***}p < 0.001$.

Results

t-LTD is induced in juvenile but not in young adult mice

We first confirmed that pairing presynaptic stimulation with single postsynaptic spikes at low frequency induces t-LTD at L4–L2/3 synapses. In slices prepared from the mouse barrel cortex at P13–27, the EPSPs evoked by extracellular stimulation of L4 axons were monitored by whole-cell recording of L2/3 pyramidal cells, as described previously (Rodríguez-Moreno and Paulsen, 2008; Rodríguez-Moreno et al., 2011, 2013; Fig. 1*A*,*B*). Accordingly, t-LTD was induced in current-clamp mode using 100 pairings of single EPSPs and single postsynaptic spikes at 0.2 Hz. A post-before-pre pairing protocol (post-pre protocol), with a postsynaptic spike occurring ~18 ms before the presynaptic stimulation, induced robust t-LTD (68 ± 5%, $n = 8$), whereas an unpaired control pathway remained unchanged (101 ± 6%, $n = 8$; Fig. 1*B*,*C*). We studied the age profile of this form of t-LTD, confirming that t-LTD can be induced until P27 (63 ± 4% at P13–19, $n = 6$; 68 ± 8% at P20–27, $n = 6$; Fig. 1*D*,*E*), as reported previously (Banerjee et al., 2009), disappearing at the end of the fourth week and during the fifth week of development (104 ± 7% at P28–37, $n = 7$; Fig. 1*D*,*E*). Changes in the timing between presynaptic and postsynaptic activity during maturation could provoke the loss of plasticity during development. We tested this hypothesis using two additional time gaps between presynaptic and postsynaptic activity as a protocol to induce t-LTD, −25 and −10 ms. As occurred with a −18 ms gap, strong t-LTD was observed at P13–27 with both a −25 and −10 ms post-pre pairing (71 ± 3%, $n = 6$, and 71 ± 5%, $n = 8$, respectively), whereas t-LTD was lost at P28–37 in both cases (95 ± 3%, $n = 7$, and 103 ± 8%, $n = 7$; Fig. 1*F*,*G*). Hence, this form of t-LTD seems to be related to a specific developmental period as it cannot be induced after that, even with different spike-timing intervals.

The developmental loss of t-LTD involves enhanced inhibition mediated by the activation of adenosine A_1 type receptors

GABAergic inhibition is an important regulator of plasticity (Paulsen and Moser, 1998), and it augments as development proceeds (Banks et al., 2002). Thus, GABAergic inhibition is involved in the developmental changes in LTP induction in the hippocampus (Meredith et al., 2003) and auditory cortex (Chun et al., 2013), and it may mediate closure of the t-LTD window in the visual cortex (Hensch, 2005). To assess whether enhanced GABAergic inhibition could account for the developmental loss of t-LTD, we repeated the t-LTD experiments at P28–37 in the presence of the $\mathrm{GABA_A}$ receptor antagonist bicuculline (10 μM) or the $\mathrm{GABA_B}$ receptor antagonist SHC50911 (20 μM). We found that t-LTD was still lost under these experimental conditions (bicuculline 92 ± 8%, $n = 7$; SHC50911 120 ± 6%, $n = 7$; Fig. 2*A*, *B*), indicating that enhanced GABAergic inhibition does not induce t-LTD loss at L4–L2/3 synapses at the end of the fourth week of development. Similarly, the presence of bicuculline (10 μM) or SHC50911 (20 μM) did not affect t-LTD at P13–27 (bicuculline 72 ± 5%, $n = 6$; SHC50911 79 ± 6%, $n = 8$, vs 63 ± 4%, $n = 9$, in untreated slices; Fig. 2*C*,*D*).

Adenosine participates in the gating of synaptic plasticity in the adult hippocampus (Arai et al., 1990; de Mendonça and Ribeiro, 1994; Rex et al., 2005; zur Nedden et al., 2011). Moreover, it has been reported that the concentration of extracellular adenosine increases during development (Sebastião et al., 2000; Rex et al., 2005; Kerr et al., 2013) and that this increase in adenosine may affect synaptic efficacy and t-LTD. In the hippocampus, it was recently found that adenosine activating presynaptic $\mathrm{A_1Rs}$ closes the windows of plasticity at CA3–CA1 synapses (Pérez-Rodríguez et al., 2019). To determine whether enhanced inhibition mediated by $\mathrm{A_1R}$ activation occurs as the somatosensory cortex matures, we assessed the effect of the $\mathrm{A_1R}$ antagonist 8-CPT (2 μM) on the EPSP slope at P13–27 and P28–37. This

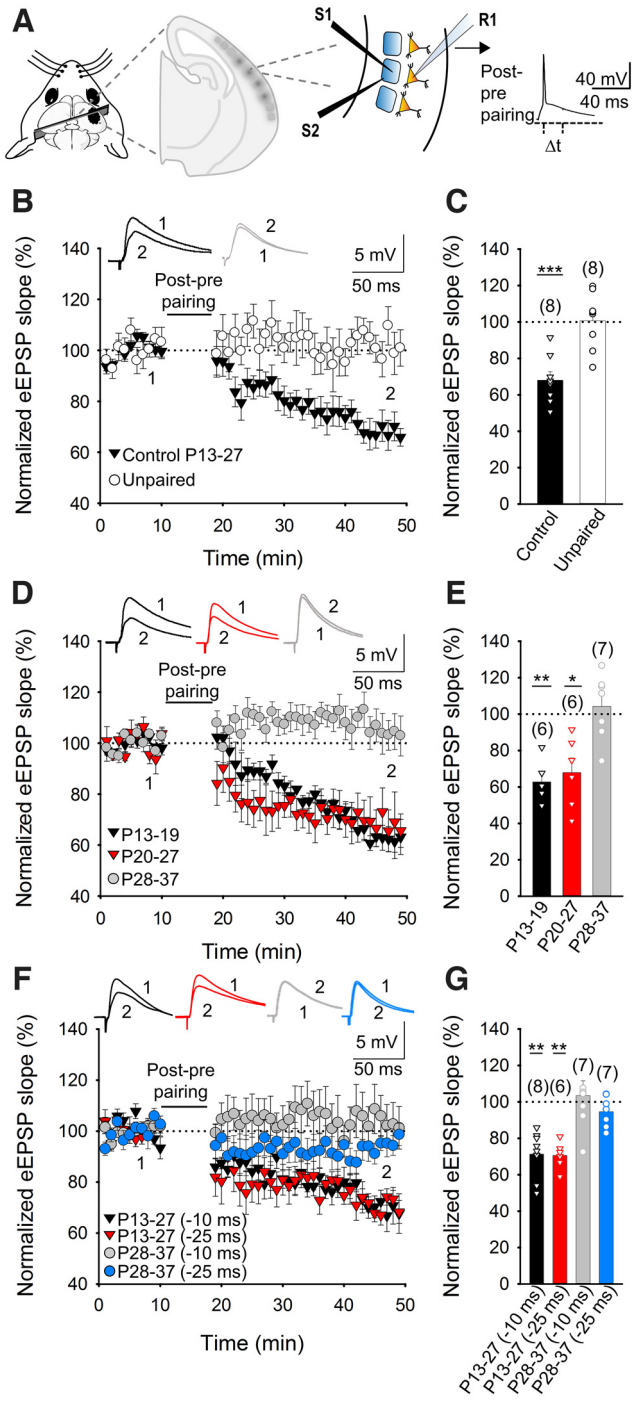

Figure 1. Input-specific spike timing-dependent LTD at L4-L2/3 synapses of the somatosensory cortex is present at P13–27 but not at P28–37. ***A***, Left, Scheme showing the general experimental setup, R, Recording electrode; S1, S2, stimulating electrodes. Right, Pairing protocol used (Δt, time between EPSP onset and peak of spike). ***B***, A post-pre-single-spike pairing protocol induced t-LTD. The EPSP slopes monitored in the paired (black triangles) and unpaired pathway (open circles) are shown. Traces show the EPSP before (1) and 30 min after (2) pairing. Depression was only observed in the paired pathway. ***C***, Summary of the results. The t-LTD is evident during the second and third week of development, but it disappears during the fourth week. ***D***, The EPSP slopes monitored at P13–19 (black triangles), P20–27 (red triangles), and P28–37 (gray circles) are shown. Traces show the EPSP before (1) and 30 min after (2) pairing. ***E***, Summary of the results. ***F***, The loss of t-LTD is not because of a shift in the coincidence time window to induce t-LTD. Using timings between presynaptic and postsynaptic activity to induce t-LTD that were shorter and longer than −18 ms (−10 and −25 ms), t-LTD is evident at P13–27 and lost at P28–37. The EPSP slopes monitored at P13–27 (black and red triangles) and P28–37 (gray and blue circles) are shown. Traces show the EPSP before (1) and 30 min after (2) pairing. ***G***, Summary of the results. Error bars indicate SEM, and the number of slices is shown in parentheses. Mann–Whitney *U test*, $*p < 0.05$, $**p < 0.01$, $***p < 0.001$.

antagonist produced a small increase in the EPSP slope at P13–27 (114 ± 5%, $n = 6$) and a robust effect at P28–37 (153 ± 8%, $n = 6$; Fig. 2*E*), indicating that A_1R activation enhances inhibition as development proceeds. By activating presynaptic A_1Rs, adenosine exerts a potent inhibitory effect on glutamatergic synaptic transmission (Dunwiddie and Masino, 2001). Thus, the loss of t-LTD at P28–37 might be because of stronger inhibition of glutamate release mediated by presynaptic A_1R activation, as recently described in the hippocampus (Pérez-Rodríguez et al., 2019). To test this, we confirmed that the effects observed were mediated by presynaptic A_1Rs by analyzing the PPR in cortical slices treated with 8-CPT (2 μM). A decrease in the PPR was observed at both P13–27 (from 1.89 ± 0.16 at baseline to 1.4 ± 0.14 in the presence of 8-CPT, $n = 6$) and P28–37 (2.01 ± 0.21% baseline, 1.44 ± 0.12 8-CPT, $n = 6$; Fig. 2*F*), indicative of a presynaptic effect. We then determined whether this increase in A_1R-mediated inhibition during development affected t-LTD, studying slices from P28–37 mice that lack t-LTD. A post-before pre protocol induced t-LTD in slices exposed to 8-CPT (2 μM; 80 ± 7% vs 106 ± 6% in interleaved control slices, $n = 8$; Fig. 2*A*,*B*), indicating that the lack of t-LTD observed was provoked by enhanced inhibition mediated by A_1R activation. In the presence of 8-CPT (2 μM), t-LTD was not affected at P13–27 (63 ± 4%, $n = 9$, in the presence and 61 ± 7%, $n = 7$, in the absence of 8-CPT; Fig. 2*C*,*D*) and, hence, the activation of presynaptic A_1Rs by adenosine appears to dampen glutamate release and prevent the induction of t-LTD.

A_1R activation at P13–P27 closes the window of plasticity

If the increase in the concentration of extracellular adenosine as development proceeds more strongly activates presynaptic A_1Rs at L4–L2/3 synapses, provoking the loss of t-LTD at P28–37, it should be possible to close the window of plasticity earlier by prematurely enhancing A_1R activation (e.g., at P13–27 when t-LTD is robust). Indeed, the induction of t-LTD was in fact impaired when slices from P13–27 animals were maintained for 1 h in the presence of the A_1R agonist (2R,3R,4S,5R)−2-(6-(cyclopentylamino)-9H-purin-9-yl)−5-(hydroxymethyl) tetrahydrofuran-3,4-diol, CPA, 30 nM (96 ± 5%, $n = 11$, vs 59 ± 6%, $n = 7$, in interleaved untreated slices; Fig. 2*G*,*H*). Hence, presynaptic A_1R inhibition during development appears to be crucial for the plastic properties of these synapses.

The developmental loss of t-LTD requires astrocyte signaling to produce an increase in adenosine levels

The role of adenosine in activating presynaptic A_1Rs and driving the developmental loss of t-LTD in the somatosensory cortex raises interest in the source of this nucleoside. It is known that equilibrative nucleoside transporters can stimulate adenosine release from neurons and that an important part of the adenosine released in the nervous system arises from extracellular metabolism of the ATP released by astrocytes (Dunwiddie and Masino, 2001; Wall and Dale, 2013). Astrocyte activation may provoke the release of glutamate (Min and Nevian, 2012) and other gliotransmitters, such as D-Serine (Andrade-Talavera et al., 2016), as well as that of ATP or adenosine (Araque et al., 2014). We investigated the possible involvement of astrocytes in the release of adenosine that activates presynaptic A_1Rs and in the subsequent loss of t-LTD during development at L4–L2/3 synapses of the barrel cortex. If ATP/adenosine released by

←

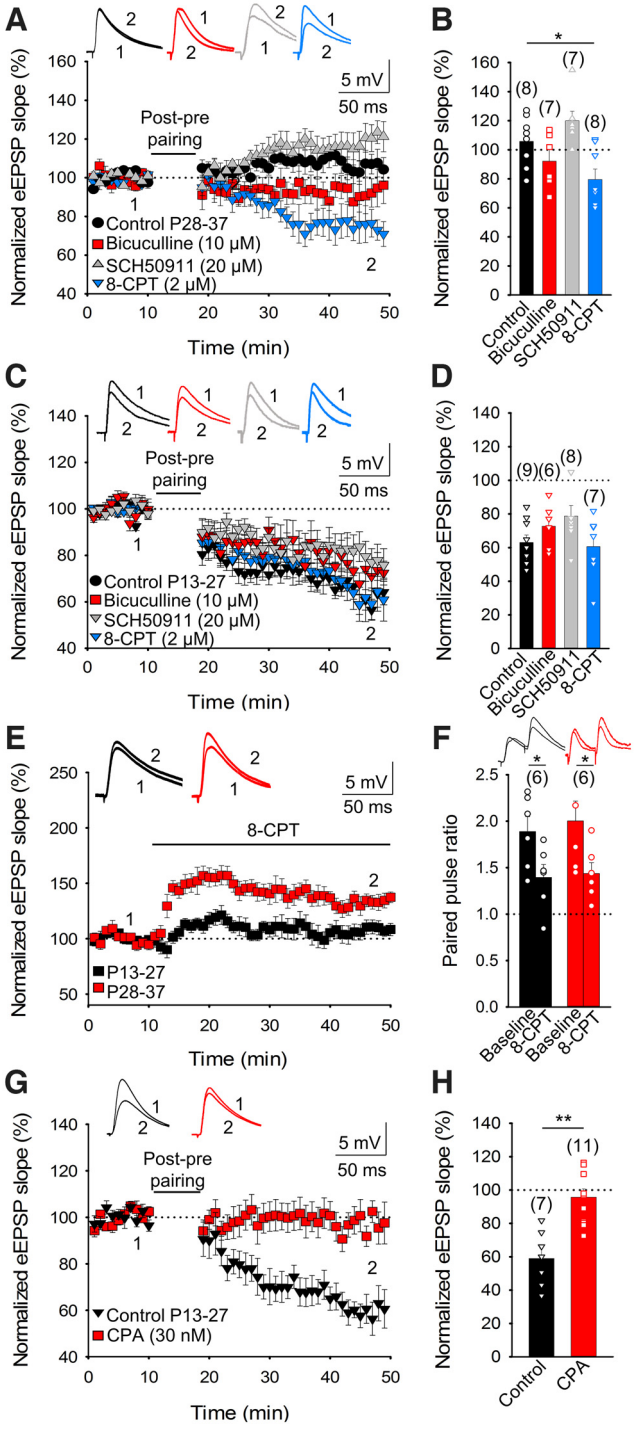

Figure 2. The developmental loss of t-LTD involves an increase in the inhibition of A1-type receptor activation by adenosine. ***A***, The loss of t-LTD is because of the activation of A1Rs and not the activation of $GABA_A$ or $GABA_B$ receptors. The t-LTD lost at P28–37 was not recovered in the presence of bicuculline (red squares) or SCH50911 (gray triangles), whereas the LTD lost is recovered completely in the presence of the A1R antagonist 8-CPT (blue triangles). Inset, The EPSP before (1) and 30 min after (2) postpairing/prepairing in control conditions (black circles) and in the presence of bicuculline (10 μM, red squares), SCH50911 (20 μM, gray triangles), or 8-CPT (2 μM, blue triangles). ***B***, Summary of the results. ***C***, At P13–27, t-LTD does not require the activation of A_1Rs, $GABA_A$, or $GABA_B$ receptors. The addition of 8-CPT (2 μM, blue triangles), bicuculline (10 μM, red triangles), or SCH50911 (20 μM, gray triangles) to the superfusion solution does not prevent t-LTD induction (black triangles). Insets, The EPSP before (1) and 30 min after (2) postpairing/prepairing. ***D***, Summary of the results. Presynaptic A1R-mediated inhibition increases with maturation. ***E***, The 8-CPT affects the evoked EPSP slope distinctly at P13–27 (black squares) and P28–37 (red squares). ***F***, Effect of 8-CPT on the PPR. Note that 8-CPT produces a decrease in the PPR at P13–27 and P28–37. An increase in A1R mediated-inhibition closes the window of plasticity for t-LTD at P13–27. ***G***, Activation of A1Rs at P13–27 by the agonist CPA prevented the induction of t-LTD. The evoked EPSP slopes monitored in control slices (black triangles) and in slices treated with the A_1R agonist CPA (30 nM, red squares) following a postpairing/prepairing are shown. The traces show the EPSP before (1) and 30 min after (2) pairing in control slices, and in slices treated with CPA. ***H***, Summary of the results. Error bars indicate SEM, and the number of slices is shown in parentheses. Kruskal–Wallis test (***B***, ***D***), Wilcoxon signed-rank test (***F***), and Mann–Whitney *U* test (***H***); $^*p < 0.05$, $^{**}p < 0.01$.

astrocytes, possibly as a result of astrocyte activation, is involved in this loss of t-LTD during development, and this ATP/adenosine is released in vesicles, impeding vesicle release by astrocytes should prevent the effects of adenosine and favor the maintenance of t-LTD. Indeed, when individual astrocytes from P28–37 mice were loaded with the Ca^{2+} chelator BAPTA (20 mM) via the patch pipette to inhibit vesicle and Ca^{2+}-dependent gliotransmitter release, t-LTD was recovered (74 ± 6%, $n = 8$, vs 106 ± 5%, $n = 8$; Fig. 3*A*,*B*,*C*). However, this recovery of t-LTD was impeded when the BAPTA-loaded astrocytes were exposed to the A_1R agonist CPA (100 ± 5%, $n = 8$; Fig. 3*B*, *C*). In addition, we tested the effect of CPA (30 nM) on basal synaptic transmission at P13–27 and P28–37, demonstrating that CPA affected the EPSP slope similarly at both stages of maturation (39 ± 6% at P13–27 and 44 ± 6% at P28–37, $n = 5$). Together, these results indicate that astrocytes and adenosine, or its precursor ATP, were responsible for the loss of t-LTD at P28–37.

To gain more insight into the role of astrocytes in the possible release of the ATP/adenosine that affects presynaptic glutamate release, we performed dual recordings in astrocytes and neighboring pyramidal neurons, monitoring the time course of the EPSP slope evoked by basal stimulation at 0.2 Hz at P13–27 and P28–37. At P13–27, direct stimulation of astrocytes (depolarization from −80 mV to 0 mV at 0.4 Hz for 10 min) produced a clear decrease in the eEPSP slope (71 ± 6%, $n = 7$; Fig. 3*D*,*E*), which was not evident in the presence of 8-CPT (2 μM; 99 ± 7%, $n = 7$; Fig. 3*D*,*E*). A decrease in the EPSP slope was also observed at P28–37 when astrocytes were stimulated (78 ± 4%, $n = 7$; Fig. 3*G*,*H*), and again, astrocyte stimulation did not affect EPSP slope in the presence of 8-CPT (98 ± 4%, $n = 7$; Fig. 3*G*,*H*). We also found a clear increase in PPRs after astrocyte stimulation at P13–27 (from 1.20 ± 0.14 at baseline to 1.70 ± 0.15, $n = 6$; Fig. 3*F*) and P28–37 (from 1.50 ± 0.25 at baseline to 1.90 ± 0.35, $n = 6$; Fig. 3*I*), indicating a presynaptic mechanism for this decrease in the EPSP slope. Together, these results indicate that the release of ATP/adenosine after astrocyte stimulation altered the probability of glutamate release through the activation of presynaptic A_1Rs, influencing the loss of t-LTD during development and closing the window of plasticity at L4–L2/3 synapses.

A switch from t-LTD to t-LTP at P38–60

A switch from t-LTD to t-LTP has been recently described in the hippocampus after t-LTD loss (Falcón-Moya et al., 2020), and, thus, we assessed whether a similar switch operates in the somatosensory cortex at L4–L2/3 synapses. We studied these synapses at older ages using a post-pre protocol, with a postsynaptic spike arising ~18 ms before the presynaptic stimulation was applied. A robust t-LTD was induced at P13–27 with this protocol, yet there was no plasticity at P28–37, whereas robust t-LTP was provoked when the protocol was applied at P38–60 (139 ± 4%, $n = 6$, vs 102 ± 5%, $n = 6$, in the

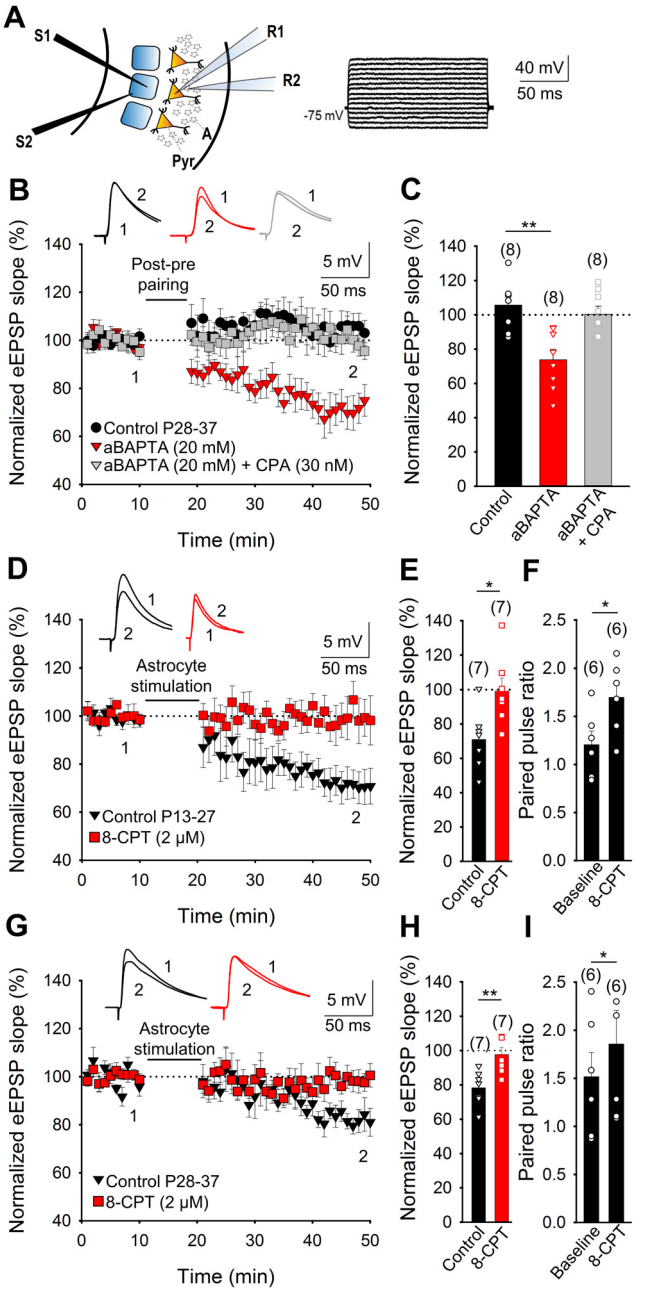

Figure 3. The adenosine involved in preventing t-LTD at P28–37 comes from astrocytes. Astrocytes are required for the loss of t-LTD with maturation. ***A***, Left, Scheme showing the general experimental setup: R1, R2, Recording electrodes; S1, S2, stimulating electrodes; Pyr, pyramidal neuron; A, astrocyte, Right, Voltage responses of an astrocyte shown in current clamp. ***B***, In astrocyte-neuron dual recordings with the astrocyte loaded with the calcium chelator BAPTA (20 mM) via the recording pipette (aBAPTA), a postpairing/prepairing protocol induces t-LTD (red triangles) yet not in control conditions (no aBAPTA, black circles). The presence of CPA (30 nM) impaired the t-LTD observed with aBAPTA (gray squares). The traces show the EPSP before (1) and 30 min after pairing (2). ***C***, Summary of the results. ***D–I***, Astrocyte stimulation affects the EPSP slope in neighboring pyramidal neurons at L4–L2/3 synapses. Performing dual recordings in astrocytes and neighboring pyramidal neurons, and monitoring the slope of EPSP evoked by basal stimulation at 0.2 Hz at P13–27 and P28–37 indicated a clear decrease in the slope of the eEPSP when the astrocyte was directly stimulated at P13–27 (depolarized from −80 mV to 0 mV at 0.4 Hz for 10 min; ***D***, ***E***). An increase in PPR was observed after astrocyte stimulation (***F***). In slices treated with 8-CPT (2 μM), astrocyte stimulation did not affect the EPSP slope (***D***, ***E***). At P28–37, a decrease in the EPSP slope was also observed in untreated slices, whereas in the presence of 8-CPT, no effect on the EPSP slope was again observed after stimulation of the astrocyte (***G***, ***H***). In the untreated slices an increase in PPR was observed after astrocyte stimulation (***I***). Error bars indicate SEM, and the number of slices is shown in parentheses. Kruskal–Wallis test (***C***), Mann–Whitney *U* test (***E***, ***H***), and Wilcoxon signed-rank test (***F***, ***I***); $*p < 0.05$, $**p < 0.01$.

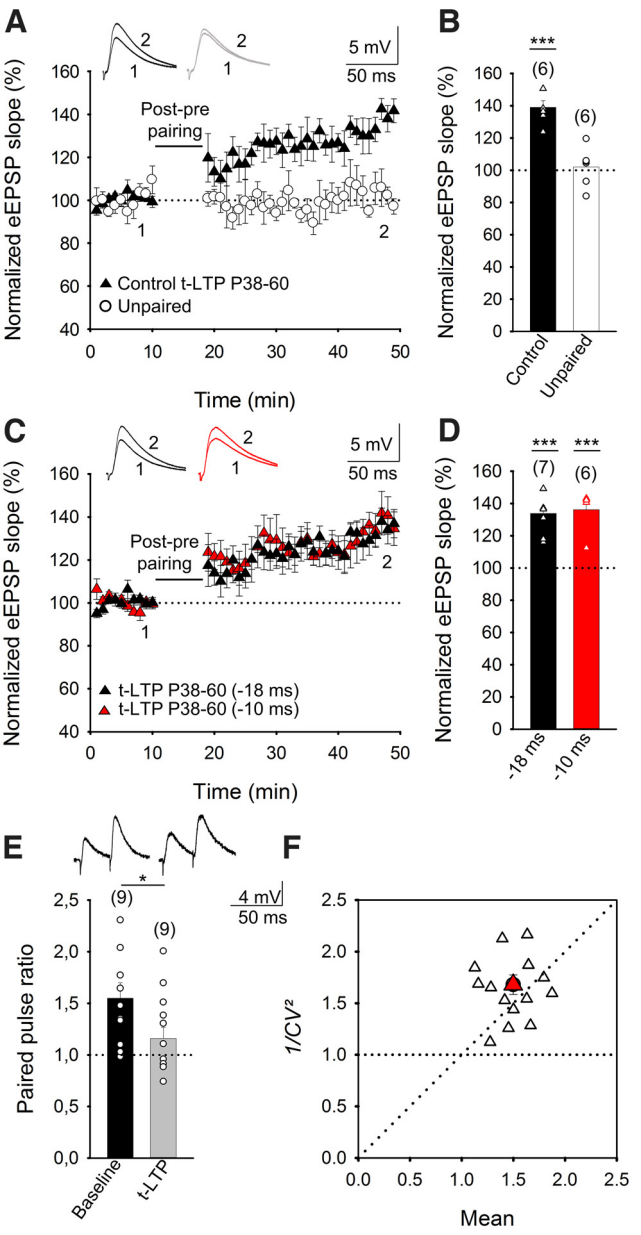

Figure 4. The presynaptic t-LTD at P13–27 in the somatosensory cortex switches to t-LTP at P38–60. ***A***, A postprotocol/preprotocol induces t-LTP at P38–60. The EPSP slopes monitored in paired (black triangles) and unpaired pathways (white circles) are shown. The traces show the EPSP before (1) and 30 min after (2) applying the induction protocol in the paired pathway, only the paired pathway showed t-LTP. ***B***, Summary of the results. ***C***, A postpairing before prepairing protocol at P38–60 induces t-LTP for $\Delta t = -18$ ms (black triangles) and $\Delta t = -10$ ms (red triangles). ***D***, Summary of results. ***E***, t-LTP induced by a postprotocol/preprotocol at P38–60 is expressed presynaptically. PPR decreases after t-LTP, sample traces at baseline and 30 min after the induction of t-LTP. ***F***, A normalized plot of $CV - 2$ versus mean EPSP slope yields data points mainly above the diagonal after induction of t-LTP. Error bars indicate SEM, and the number of slices is shown in parentheses. Mann–Whitney *U* test (***B***, ***D***) and Wilcoxon signed-rank test (***E***); $***p < 0.001$, $*p < 0.05$.

unpaired pathway; Fig. 4*A*,*B*). Hence, there appears to be a switch from t-LTD to t-LTP at L4–2/3 synapses of somatosensory cortex during development. To determine whether the switch observed also occurred with other time intervals between spikes, we performed experiments using a −10 ms gap. A switch to t-LTP was also observed at −10 ms (post-pre protocol 136 ± 6%, $n = 6$; Fig. 4*C*,*D*) as occurred at −18 ms (134 ± 5%, $n = 7$; Fig. 4*C*,*D*), indicating the switch

from t-LTD to t-LTP is common to at least two different spike time intervals (−18 and −10 ms).

Presynaptic expression of t-LTP

Although t-LTD is known to be presynaptically expressed at S1 L4–L2/3 synapses (Bender et al., 2006; Nevian and Sakmann, 2006; Brasier and Feldman, 2008; Rodríguez-Moreno and Paulsen, 2008; Rodríguez-Moreno et al., 2011; but see Carter and Jahr, 2016), we confirmed that here by analyzing the paired-pulse facilitation ratio and CV. First, we analyzed the PPRs at baseline and 30 min after the pairing protocol was applied, identifying a significant decrease in the PPR after t-LTP (from 1.55 ± 0.15 at baseline to 1.16 ± 0.11, $n = 9$; Fig. 4*E*) that was indicative of a presynaptic change. Second, we estimated the noise-subtracted CV of the synaptic responses before and after t-LTP induction. A plot of CV^{-2} versus the change in the mean evoked EPSP slope (M) before and after t-LTP mainly yielded points above the diagonal line, consistent with a presynaptic modification of release parameters (Brock et al., 2020; Fig. 4*F*). Together, these data suggest an increase in the probability of neurotransmitter release in the paired pathway, and they are indicative of a presynaptic locus for this form of t-LTP.

Presynaptic t-LTP requires NMDARs and mGluRs

The t-LTD detected in juveniles (P13–27) requires NMDARs (Bender et al., 2006; Nevian and Sakmann, 2006; Brasier and Feldman, 2008; Rodríguez-Moreno and Paulsen, 2008; Banerjee et al., 2009, 2014; Rodríguez-Moreno et al., 2011), and, indeed, the presynaptic form of t-LTP that appears at P38–60 was prevented in the presence of D-AP5 (50 µM; 106 ± 10%, $n = 7$) or MK-801 (500 µM; 87 ± 7%, $n = 6$) relative to the interleaved controls (141 ± 5%, $n = 9$; Fig. 5*A*,*B*). Hence, the t-LTP induced by a post-pre protocol at P38–60 does require NMDARs. Because mGluRs have been implicated in plasticity and LTP in different regions and at distinct synapses (Anwyl, 2009), we tested whether the presynaptic t-LTP at L4–L2/3 synapses also required mGluRs. Indeed, t-LTP was completely blocked by exposure to the broad-spectrum mGluR antagonist LY341495 (100 µM, 94 ± 10%; $n = 6$; Fig. 5*C*,*D*) and by treating the slices with the mGluR1 antagonist LY367385 (100 µM; 113 ± 8%, $n = 7$), relative to interleaved slices for the two experimental conditions pooled together (146 ± 5%, $n = 7$; Fig. 5*C*,*D*), indicating this t-LTP required mGluR1s. To determine whether these mGluRs are postsynaptic, we repeated the experiments with the postsynaptic neuron loaded with GDPβS to prevent G-protein mediated signaling, a situation that prevented the induction of t-LTP (101 ± 10%, $n = 8$, vs 137 ± 4%, $n = 7$, in interleaved control slices with no GDPβS loaded into the postsynaptic cells; Fig. 5*E*,*F*). Hence, mGlu1R, possibly located in postsynaptic neurons, seems to be necessary for t-LTP induction.

Presynaptic t-LTP requires postsynaptic Ca^{2+} and NO

Both t-LTP and t-LTD appear to require postsynaptic Ca^{2+} at neocortical (Bender et al., 2006; Nevian and Sakmann, 2006; Rodríguez-Moreno et al., 2013) and hippocampal synapses (Andrade-Talavera et al., 2016; Falcón-Moya et al., 2020; Mateos-Aparicio and Rodríguez-Moreno, 2020), which led us to assess whether the presynaptic t-LTP at cortical L4–L2/3 synapses also requires postsynaptic Ca^{2+}. When we loaded the postsynaptic neuron with the calcium chelator BAPTA (20 mM), t-LTP was not induced (101 ± 6%, $n = 6$; Fig. 6*A*,*B*), demonstrating that postsynaptic calcium was

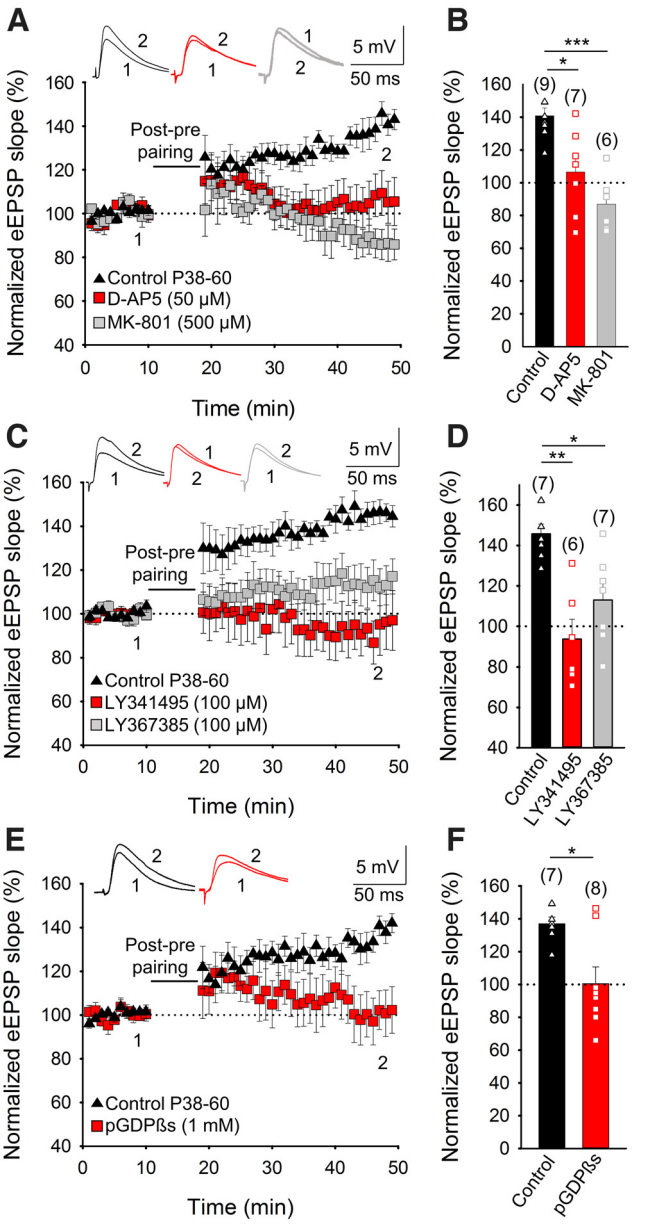

Figure 5. Presynaptic t-LTP requires NMDA and Group I mGluR1 metabotropic glutamate receptors. ***A***, Addition of D-AP5 (50 µM) or MK-801 (500 µM) to the superfusion solution prevented t-LTP induction. The EPSP slope is shown in D-AP5-treated (red squares), MK-801-treated (gray squares), and untreated cells (black triangles). The traces show the EPSP before (1) and 30 min after (2) pairing. ***B***, Summary of the results. ***C***, The t-LTP requires mGluR. The EPSP slopes monitored in control slices (black triangles) and in slices treated with the mGluR antagonist LY341495 (100 µM, red squares) or the mGluR1 antagonist LY367385 (100 µM, gray squares) are shown following postpairing before prepairing. The traces show the EPSP before (1) and 30 min after (2) pairing. ***D***, Summary of the results. ***E***, The t-LTP requires activation of postsynaptic mGluRs. Time course of t-LTP induction in control conditions (black triangles) and with the postsynaptic neuron (red squares) loaded with GDPβS (1 mM). Inset, Traces show the EPSP before (1) and 30 min after pairing (2) in control slices or when the postsynaptic neurons are loaded with GDPβS. ***F***, Summary of the results. Error bars indicate SEM, and the number of slices is shown in parentheses. Kruskal–Wallis test (***B***, ***D***) and Mann–Whitney *U* (***F***); $^*p < 0.05$, $^{**}p < 0.01$, $^{***}p < 0.001$.

required for t-LTP. As L-type Ca^{2+} channels have been implicated in plasticity in the cortex (Bender et al., 2006; Nevian and Sakmann, 2006), we evaluated whether they were involved in t-LTP by performing the pairing protocol after bath application of the L-type Ca^{2+} channel blocker nimodipine (10 µM). In these conditions t-LTP was prevented

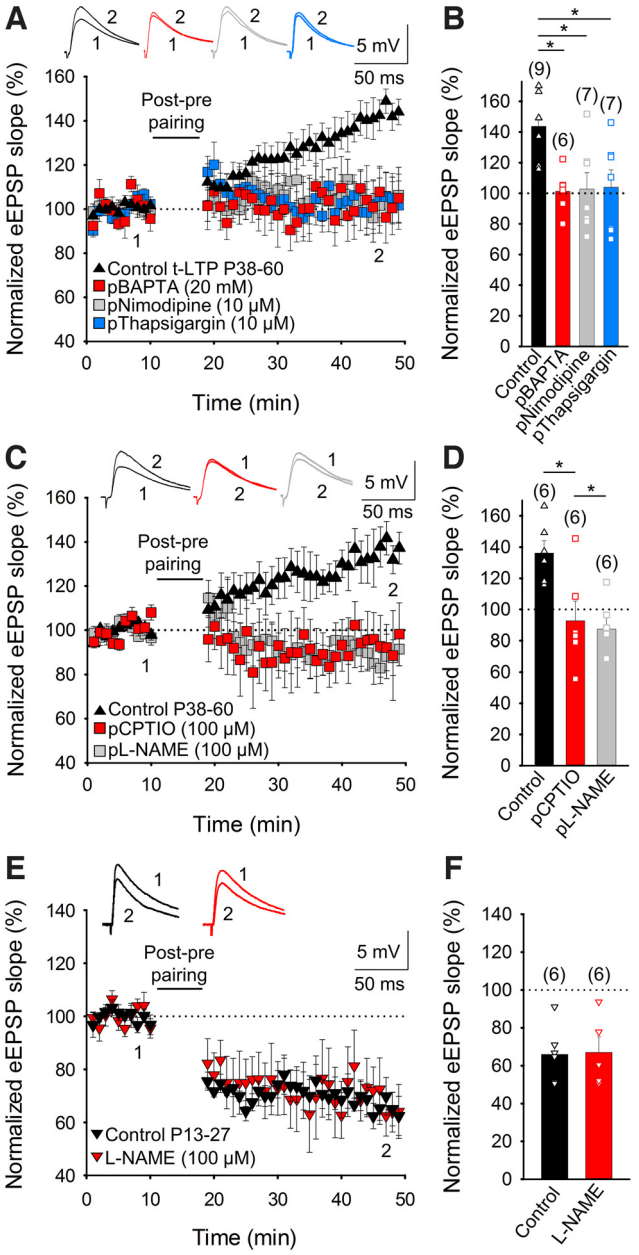

Figure 6. Postsynaptic calcium and NO are required for t-LTP. ***A***, t-LTP is prevented by loading BAPTA (20 mM), nimodipine (10 μM), and thapsigargin (10 μM) into the postsynaptic recording pipette. The EPSP slopes shown were monitored in control slices (black triangles) and in slices treated with BAPTA (red squares), nimodipine (gray squares), or thapsigargin (blue squares). The traces show the EPSP before (1) and 30 min after (2) pairing. ***B***, Summary of the results. ***C***, Time course of the effect of postpairing before prepairing in control conditions (black triangles) and loading cPTIO (100 μM, red squares) or L-NAME (100 μM, gray squares) into the postsynaptic neuron. Insets, The traces show the EPSPs before (1) and 30 min after pairing (2). ***D***, Summary of the results. Error bars indicate SEM, and the number of slices is shown in parentheses. NO is not necessary for t-LTD at P13–P27. ***E***, The EPSP slopes monitored in control conditions (black triangles) and in the presence of L-NAME (100 μM, red triangles) are shown. Traces show the EPSP before (1) and 30 min after (2) pairing for each condition. ***F***, Summary of the results. Error bars indicate SEM, and the number of slices is shown in parentheses. Kruskal–Wallis test, $^*p < 0.05$.

(111 ± 7%, $n = 7$), as it was when nimodipine was loaded into the postsynaptic neuron (103 ± 10%, $n = 7$; Fig. 6*A*,*B*), indicating that like presynaptic t-LTD, this presynaptic t-LTP requires calcium flux through L-type calcium channels into the postsynaptic neuron. In addition, the release of Ca^{2+} from intracellular stores is thought to be required for plasticity at cortical and hippocampal synapses (Bender et al., 2006; Nevian and Sakmann, 2006; Andrade-Talavera et al., 2016; Falcón-Moya et al., 2020). Indeed, when we assessed this possibility, t-LTP was prevented when the post-pre protocol was applied at P38–60 after depleting intracellular Ca^{2+} stores by loading the postsynaptic neuron with thapsigargin (10 μM; 104 ± 11%, $n = 7$, vs interleaved controls, 144 ± 6%, $n = 9$; Fig. 6*A*,*B*). Hence, Ca^{2+} release from intracellular stores is required for t-LTP.

It was recently demonstrated that NO from the postsynaptic neuron is necessary to induce presynaptic t-LTP in the hippocampus (Falcón-Moya et al., 2020). NO has been identified as a retrograde signal implicated in presynaptic LTP (Castillo, 2012; Pigott and Garthwaite, 2016; Padamsey et al., 2017), and there is evidence that calcium influx through L-type calcium channels could participate in NO synthesis and/or its release from postsynaptic neurons (Parpura and Zorec, 2010; Castillo, 2012). The induction of presynaptic t-LTP was prevented when the NO scavenger cPTIO (100 μM; 93 ± 12%, $n = 6$) or the NO synthase inhibitor L-NAME (100 μM; 87 ± 7%, $n = 6$) was loaded into the postsynaptic neuron, relative to the presynaptic t-LTP in interleaved controls (136 ± 8%, $n = 6$; Fig. 6*C*,*D*). Interestingly, L-NAME had no effect on t-LTD when added to the bath at P13–27 (67 ± 8%, $n = 6$, vs 66 ± 6%, $n = 6$, in interleaved controls; Fig. 6*E*,*F*). Together, these results indicate that NO produced and released by the postsynaptic neuron is required specifically for t-LTP.

Presynaptic t-LTP involves astrocytic signaling

Astrocytes are implicated in t-LTD at the synapses studied here (Min and Nevian, 2012; Rodríguez-Moreno et al., 2013), and they participate in closing the window of plasticity as the hippocampus matures. Thus, we assessed whether astrocyte activation is also necessary to induce the presynaptic form of t-LTP that appears after P38. When individual astrocytes in slices from P38–60 mice were loaded with the Ca^{2+} chelator BAPTA (20 mM) through the patch pipette to inhibit vesicle and Ca^{2+}-dependent gliotransmitter release (Pascual et al., 2005), no t-LTP was observed at proximal (50–100 μm) L4–L2/3 synapses (105 ± 9%, $n = 9$; Fig. 7*A*,*B*). Moreover, this phenomenon was assessed in P38–60 dn-SNARE mutant mice in which vesicular gliotransmitter release is blocked (Pascual et al., 2005; Sardinha et al., 2017). In slices from dn-SNARE mice, the basal activity of L4–L2/3 synapses was slightly stronger (23 ± 8%, $n = 7$) because of the lack of ATP/adenosine tonic inhibition, and less intense stimulation was necessary to obtain the same amplitude EPSP as in slices from WT mice, as reported previously in other regions (Pascual et al., 2005; Sardinha et al., 2017). In these mutant mice, the typical t-LTP observed at P38–60 in WT L4–L2/3 synapses (148 ± 7%, $n = 9$) was not evident (83 ± 5%, $n = 7$; Fig. 7*A*,*B*). Together, these results indicate that astrocytes are required for t-LTP induction and for the switch from t-LTD to t-LTP.

Enhanced inhibition of presynaptic release mediated by the activation of A_1Rs is involved in t-LTP. Having demonstrated that presynaptic A_1R activation is responsible for the loss of t-LTD at P28–37, we found that the antagonist of A_1Rs (8-CPT) also fully impaired t-LTP (68 ± 6%, $n = 6$, vs 140 ± 3%, $n = 6$, in interleaved control slices; Fig. 7*C*,*D*). Although 8-CPT did not affect t-LTD at P13–27 (Fig. 2*C*,*D*), it did still recover the lost t-LTD at P28–37 (Fig. 2*A*,*B*). When the EPSP slope was measured in the presence of this A_1R antagonist, 8-CPT had a stronger effect at P28–37 than at P13–27 (Fig. 2*E*,*F*). If extracellular

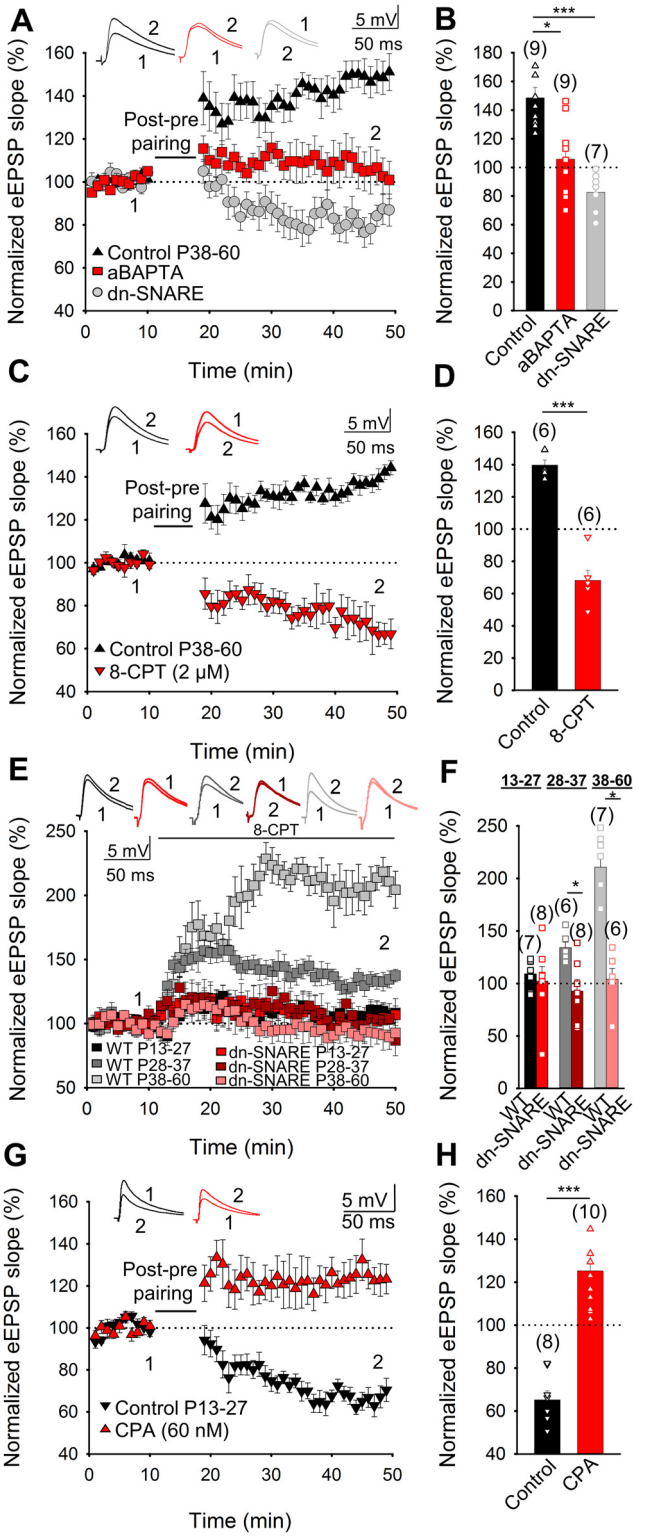

Figure 7. The involvement of astroglial adenosine in t-LTP. ***A***, Astrocytes are required for t-LTP. Time course of t-LTP induction in control conditions (black triangles), and of the loss of t-LTP in BAPTA-treated astrocytes (20 mM, red squares) or in dnSNARE mutant mice (gray circles). The traces show the EPSP before (1) and 30 min after pairing (2). ***B***, Summary of the results. ***C***, Time course of t-LTP induction in control conditions (black triangles) and of the loss of t-LTP in 8-CPT-treated slices (2 μM, red triangles). The traces show the EPSP before (1) and 30 min after pairing (2). ***D***, Summary of the results. ***E***, 8-CPT increases the evoked EPSP slope at P13–27 (black squares), P28–37 (dark gray squares), and P38–60 (light gray squares) in WT but not in dn-SNARE mice (P13–27, red squares; P28–37, dark red squares; P38–60, light red squares). ***F***, Summary of the results. ***G***, An increase in presynaptic A1R mediated inhibition converts t-LTD at P13–27 in t-LTP. When A1Rs are activated by CPA (60 nM) at P13–27, a post-pre protocol induced t-LTP. The EPSP slopes monitored in the control condition (black triangles) and in the presence of bath-applied CPA (red triangles) are shown. The traces show the EPSP before (1) and 30 min after (2) pairing. ***H***, Summary of results. Error bars indicate SEM, and the number of slices is shown in parentheses. Kruskal–Wallis test (***B***) and Mann–Whitney test (***D***, ***F***, ***H***); *$p < 0.05$, ***$p < 0.001$.

adenosine levels continue to increase as development proceeds, a stronger effect on presynaptic A_1Rs would be expected at P38–60. Indeed, the EPSP slope increased more in the presence of 8-CPT at this later age (P38–60 218 ± 10%, $n = 7$) than at P13–27 (117 ± 4%, $n = 7$) or P28–37 (150 ± 8%, $n = 6$; Fig. 7*E*,*F*). These results indicate that presynaptic A_1R mediated inhibition increases with maturation. We also studied the effect of 8-CPT in dn-SNARE mice to determine whether the ATP/adenosine that activates A_1Rs originates from astrocytes, and we found that 8-CPT had practically no effect on the EPSP slope in these mice at any of the ages studied (P13–27 115 ± 6%, P28–37, $n = 8$; 112 ± 9%, $n = 8$; and P38–60 115 ± 12%, $n = 6$. Fig. 7*E*,*F*).

A_1R activation at P13–27 converts t-LTD into t-LTP. If extracellular adenosine concentrations increase during development and more strongly activate presynaptic A_1R at L4–L2/3 cortical synapses, dampening the glutamate release and mediating a switch from t-LTD to t-LTP at P38–60, it might be possible to convert t-LTD to t-LTP earlier in the development by enhancing A_1R activation (e.g., at P13–27 when t-LTD is robust or at P28–37 when t-LTD is lost). We previously demonstrated that CPA (30 nM) cannot convert t-LTD into t-LTP, but rather it prevents t-LTD induction at P13–27 (Fig. 2*E*,*F*). However, increasing the concentration of CPA to 60 nM converted t-LTD into t-LTP at P13–27 (from 65 ± 4%, $n = 8$, to 125 ± 7%, $n = 10$; Fig. 7*G*,*H*). These results were consistent with a primary involvement of A_1Rs in the switch from t-LTD to t-LTP associated with maturation, and they suggest that the adenosine activating A_1Rs might be released by astrocytes. As such, presynaptic adenosine activated presynaptic A_1Rs, an effect that was enhanced as the brain matures.

Adenosine and glutamate are required for t-LTP

It might be expected that if ATP/adenosine was the only gliotransmitter mediating the switch from t-LTD to t-LTP, the A_1R agonist CPA should be able to recover t-LTP at P38–60 in dn-SNARE mice when no t-LTP would otherwise be observed. However, t-LTP was not recovered by CPA in these conditions (105 ± 8%, $n = 6$, vs 149 ± 7%, $n = 9$, in control slices; Fig. 8*A*,*B*), suggesting that another gliotransmitter released by astrocytes or just after astrocyte activation might also be involved. We tested whether glutamate may also be required to induce presynaptic t-LTP at P38–60 by applying glutamate puffs. When we tested this in slices from dn-SNARE mice maintained in the presence of CPA, the glutamate puffs applied partially recovered the t-LTP (122 ± 6%, $n = 6$; Fig. 8*A*,*B*), indicating that the ATP/adenosine and glutamate, probably released as gliotransmitters by astrocytes, seem to be necessary for the induction of presynaptic t-LTP.

Finally, to define the signal that might stimulate astrocytes to release gliotransmitters and mediate this form of LTP, we evaluated the role of NO, the release of which from the postsynaptic neuron is necessary for t-LTP. NO was previously shown to increase the calcium that enters and stimulates astrocytes (Matyash et al., 2001), raising the possibility that NO could

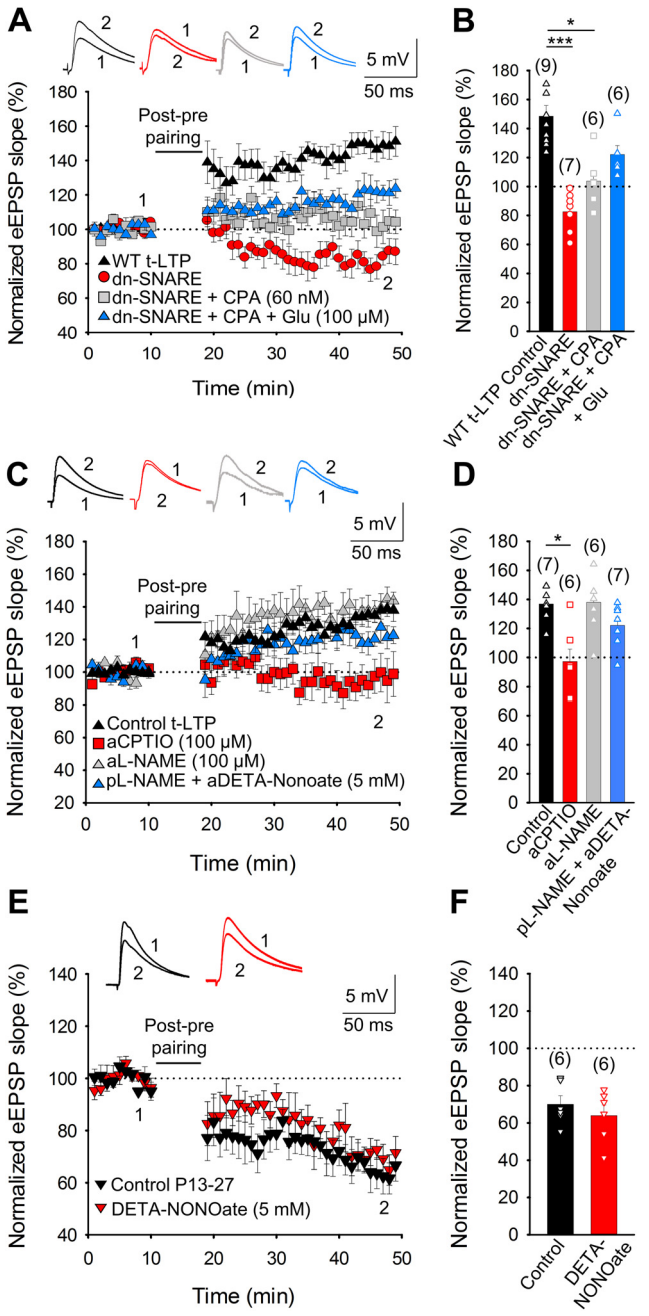

Figure 8. Astroglial glutamate involvement in t-LTP. ***A***, The release of glutamate and adenosine by astrocytes is necessary for presynaptic t-LTP induction. Time course of the effect of postpairing before prepairing in control conditions (black triangles), in dn-SNARE slices (red circles), in slices from dn-SNARE mice exposed to CPA (60 nM, gray squares), or in slices from dn-SNARE mice exposed to CPA and glutamate puffs (100 μM, blue triangles). Insets, The traces show the EPSPs before (1) and 30 min after pairing (2). ***B***, Summary of the results. NO is necessary for astrocyte release of gliotransmitter(s) and t-LTP induction. ***C***, t-LTP is prevented by loading CPTIO (100 μM) into the astrocyte via the recording pipette but not by loading L-NAME (100 μM). When L-NAME is loaded into the postsynaptic neuron and NO donor (DETA-NONOate, 5 mM) added in forms of puffs over astrocytes, t-LTP is partially recovered. The EPSP slopes monitored are shown in paired control slices (black triangles) and in slices treated with aCPTIO (red squares), aL-NAME (gray triangles) and pL-NAME + DETA-NONOate (blue triangles). The traces show the EPSP before (1) and 30 min after (2) pairing. ***D***, Summary of the results. Error bars indicate SEM, and the number of slices is shown in parentheses. The NO donor, DETA-NONOate, does not affect t-LTD at P13–27. ***E***, The EPSP slopes monitored in control conditions (black triangles) and in slices exposed to DETA-NONOate (5 mM, red triangles) are shown. Traces show the EPSP before (1) and 30 min after (2) pairing. ***F***, Summary of the results. Error bars indicate SEM, and the number of slices is shown in parentheses. Kruskal–Wallis test (***B***, ***D***); * $p < 0.05$, *** $p < 0.001$.

activate or interact with astrocytes to release ATP/adenosine and/or glutamate in our conditions. Interestingly, t-LTP induction was prevented by loading astrocytes with the NO scavenger cPTIO (96 ± 10%, $n = 6$) but not when they were loaded with L-NAME (aL-NAME 135 ± 9%, $n = 6$, vs untreated control slices 137 ± 4%, $n = 7$; Fig. 8*C*,*D*). In addition, when t-LTP induction was prevented by loading the postsynaptic neuron with L-NAME, puffs of the NO donor DETA NONOate (5 mM) on astrocytes recovered t-LTP (122 ± 6%, $n = 6$; Fig. 8*C*,*D*), although DETA-NONOate did not affect t-LTD at P13–27 (DETA-NONOate 64 ± 6%, $n = 6$, vs untreated control slices 70 ± 5%, $n = 6$; Fig. 8*E*,*F*). Hence, the NO that participated in this form of t-LTP was not synthetized by astrocytes, but rather it originated in the postsynaptic neuron.

Discussion

Loss of t-LTD by the end of the fourth week of postnatal development

Using a postprotocol/preprotocol, with a −18 ms gap between the presynaptic and postsynaptic activity, presynaptically expressed t-LTD was observed at L4–2/3 synapses from P13 to 27 (Fig. 9*A*) that disappears at ~P27, as detected previously (Banerjee et al., 2009). This is also consistent with previous studies showing that the capacity for synaptic depression at cortical synapses and in the hippocampus declines with age (Bear and Abraham, 1996; Corlew et al., 2007; Banerjee et al., 2009; Rodríguez-Moreno et al., 2013; Andrade-Talavera et al., 2016; Pérez-Rodríguez et al., 2019). There was a loss of t-LTD with two additional time gaps between presynaptic and postsynaptic activity to induce t-LTD (−25 and −10 ms), with t-LTD disappearing at P28–37. We did not check other intervals but these results are indicative that a shift in the time windows does not mediate the loss of t-LTD associated with maturation. These results extend the developmental loss of t-LTD observed in other brain regions like the visual cortex and hippocampus to the somatosensory cortex. Whether this a general phenomenon requires studying other brain regions and synapses.

Adenosine A_1 type receptors mediate the enhanced inhibition that is responsible for the loss of plasticity during development

We show that enhanced inhibition is required to close the window of plasticity. This enhanced inhibition is not mediated by $GABA_A$ receptor activation, as in the visual cortex (Hensch, 2004, 2005) where astrocytes were recently implicated in closing the critical period of plasticity (Ribot et al., 2021). Likewise, $GABA_B$ receptors do not appear to be involved in this shift (this study) because the loss of t-LTD at the end of the fourth week of development is not affected by the presence of $GABA_A$ or $GABA_B$ receptor antagonists. However, t-LTD does not disappear during development in the presence of an A_1R antagonist, a clear indication of the crucial role of adenosine in t-LTD. Indeed, activating A_1Rs at P13–27 when a robust t-LTD can be induced, the window of plasticity closed prematurely, and there was a loss of t-LTD similar to that observed in older mice (P27–38). This mechanism is similar to that observed recently in the hippocampus (Falcón-Moya, 2020), suggesting the two structures use a similar mechanism to close a window of plasticity. It will be of interest to study these mechanisms in other brain structures and synapses to confirm whether this a general mechanism in the brain.

Presynaptic A_1R activation produces a decrease in glutamate release, the most probably explanation for the loss of t-LTD

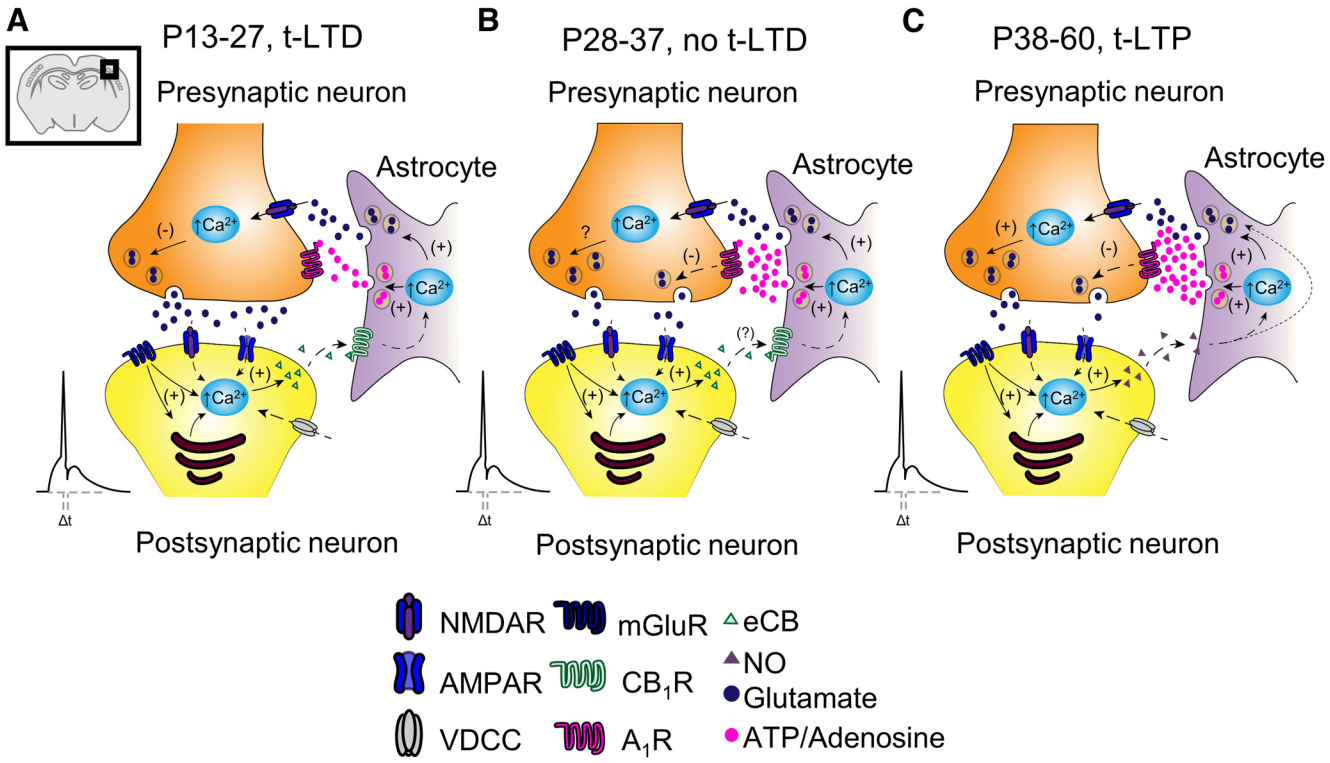

Figure 9. Scheme of the differences in signaling between early (P13–27), juvenile (P28–37), and adult (P38–60) stages of development at L4–L2/3 synapses of the somatosensory cortex. ***A***, ***B***, At P13–27, a known presynaptic form of t-LTD is induced by a post- pre-single-spike-pairing protocol. In this presynaptically expressed form of t-LTD, postsynaptic action potentials activate voltage-dependent Ca^{2+} channels (VDCCs), and the presynaptically released glutamate activates postsynaptic mGluR, provoking Ca^{2+} release from internal stores and eCB synthesis. For t-LTD, eCB is necessary to activate CB_1 receptors and to facilitate glutamate release from astrocytes. Together with the glutamate released from presynaptic neurons, this glutamate is known to activate preNMDARs on L4 boutons, leading to an increase in presynaptic Ca^{2+} and synaptic depression (Bender et al., 2006; Rodríguez-Moreno and Paulsen, 2008; Min and Nevian, 2012). In the present study, we show that t-LTD does not develop at P28–37 (***B***) and that the main difference with regard to P13–27 is an increase in adenosine release from astrocytes at this stage of development. ***C***, At P38–60 t-LTD is not only lost, but it switches to a presynaptic form of t-LTP. For the induction of this presynaptic form of t-LTP, postsynaptic action potentials activate VDCCs, inducing calcium release from internal stores and NO synthesis. The NO activates astrocytes and provokes the release of glutamate and/or adenosine, which in turn stimulates NMDARs and A_1Rs on L4 boutons, respectively. A_1R activation considerably dampens the probability of neurotransmitter release, whereas NMDAR activation produces a long-lasting increase in glutamate release and synaptic potentiation.

(Dunwiddie and Masino, 2001). Here, we used two different approaches to determine whether adenosine acts on A_1Rs, PPR, and fluctuation analysis, both of which were consistent with the presynaptic activity of A_1Rs. As observed in the hippocampus (Sebastião et al., 2000; Rex et al., 2005; Kerr et al., 2013; Falcón-Moya, 2020), the concentration of adenosine at S1 L4–L2/3 synapses seems to increase with maturation as a stronger increase in the EPSP slope was induced by 8-CPT at P28–37 than at P13–27. Thus, like CA3–CA1 synapses in the hippocampus, it seems that the activation of presynaptic A_1Rs augments during development because of the increase in extracellular adenosine. This activation inhibits glutamate release, reducing the ambient glutamate and possibly dampening the NMDAR activity necessary for t-LTD, causing its loss. Hence, the increase in adenosine seems to affect glutamate release and t-LTD (Fig. 9*B*).

Adenosine released as a result of astrocyte signaling is required for the loss of plasticity during development

It is of interest to identify the specific source of adenosine as there are many possibilities. It may be released from neurons by exocytosis (Klyuch et al., 2012) or via transporters (Lovatt et al., 2012), indirectly through the extracellular metabolism of the ATP exocytosed by neurons (Jo and Schlichter, 1999) or glial cells (Pascual et al., 2005), or through glial gap junction hemi-channels (Huckstepp et al., 2010). Indeed, these mechanisms may also operate concomitantly. We assessed whether astrocytes are needed to produce the adenosine that activates A_1Rs as they are a well-known potential source of adenosine (mostly in the form of its precursor, ATP) and other gliotransmitters, released after calcium mobilization of astrocytic vesicles (Araque et al., 2014). At P28–37, preventing vesicle release by loading astrocytes with BAPTA recovers t-LTD, an effect that was blocked by CPA, demonstrating that adenosine released by astrocytes or as a result of astrocyte signaling is required for the loss of t-LTD. Although only one astrocyte was loaded with BAPTA, the effect on plasticity observed is most probably because of the activation of a network of astrocytes, as the single cell loaded is connected to others through gap junctions (Mederos et al., 2018). We also demonstrate that directly stimulating astrocytes increases the extracellular adenosine sufficiently to affect the EPSP slope, thereby affecting glutamate release. Whether the increase in extracellular adenosine observed with maturation (here and previously in the hippocampus) is produced by an increase in the number of astrocytes or by enhanced release requires further study. Our results indicate that t-LTD is present at L4–L2/3 synapses of the mouse somatosensory cortex until the end of the fourth week of development. The disappearance of this form of t-LTD is because of inhibition mediated by the activation of presynaptic A_1Rs during maturation. The involvement of adenosine in closing windows of plasticity is emerging as a common regulatory event given that it has also been seen in

the hippocampus (Pérez-Rodríguez et al., 2019), and adenosine has been seen to be able to recover plasticity at a systems level in the adult auditory cortex (Blundon et al., 2017).

A switch from t-LTD to t-LTP occurs at P38–60

In the second part of this study, we show that presynaptic t-LTD switches to presynaptic t-LTP at somatosensory L4–L2/3 synapses as young mice mature, demonstrating that this form of t-LTP is expressed presynaptically and that it requires mGluR1 and NMDAR activation. In addition, this presynaptic t-LTP requires the flux of calcium through postsynaptic L-type calcium channels, as well as calcium release from postsynaptic intracellular stores and postsynaptic NO release. The latter acts as a retrograde signal that mediates the astroglial release of ATP/adenosine to activate presynaptic A_1Rs and that of glutamate to presumably activate NMDARs (Fig. 9*C*). We present evidence from two approaches to determine the locus of this form of t-LTP, PPRs and CV, both consistent with presynaptic changes. Hence, this presynaptically expressed LTP appears during development through a switch from t-LTD such that our findings expand the repertoire of presynaptic LTPs to this type at S1 L4–L2/3 synapses. Studying the timing dependency of this form of t-LTP, the switch from t-LTD to t-LTP occurred at different time intervals, −18 and −10 ms, where there was robust t-LTD at P13–27. Hence, this switch would appear to arise on maturation, and it is most probably not because of a broadening of the time interval or a shift along the time axis, although it is possible that the switch does not happen at time intervals not tested. A relevant question that needs to be addressed is whether this switch from t-LTD to t-LTP is observed only with STDP or if it is also present when other protocols are used that induce LTD in young animals. It is noteworthy that STDP has been suggested to depend on the extracellular calcium concentration ($[Ca^{2+}]_e$) in the hippocampus, where at $[Ca^{2+}]$e considered to be physiological (1.3–1.8 mM) t-LTD plasticity alone was impaired (Inglebert et al., 2020). In the somatosensory cortex studied, the $[Ca^{2+}]$e is slightly higher than the indicated interval (2 mM), and, interestingly, both t-LTD and the switch to t-LTP occur in the presence of 1.5 mM or 2 mM $[Ca^{2+}]$e, suggesting that both effects will be produced under physiological Ca^{2+} concentrations. This is also consistent with the fact that t-LTD at somatosensory cortex L4–L2/3 synapses has been witnessed *in vivo* in young mice (González-Rueda et al., 2018). Thus, it would be particularly interesting to determine whether this switch from t-LTD to t-LTP occurs *in vivo*.

Presynaptic t-LTP requires NMDAR and mGluR1

Regarding the receptor systems necessary for presynaptic t-LTP to appear as the animal matures, some clear differences were found between the hippocampus and somatosensory cortex. Although both types of t-LTP are presynaptically expressed, t-LTP requires NMDARs at L4–L2/3 synapses but not in the hippocampus. This is an interesting difference as a decrease in the number of presynaptic NMDARs has been found in the visual cortex with maturation (Corlew, 2007) and hippocampus (Pérez-Rodríguez et al., 2019). Although a possible switch from presynaptic t-LTD to presynaptic t-LTP has not yet been described in the visual cortex, it is associated with a lack of presynaptic NMDAR activity in the hippocampus. This probably indicates that the number of NMDARs is too low, and they cannot therefore participate in t-LTP, with mGluR5 participating instead (Pérez-Rodríguez et al., 2019; Falcón-Moya et al., 2020). Future experiments will determine whether changes in the number of preNMDARs also occurs at S1 L4–L2/3 synapses with maturation. It is also possible that there is a different time course for hippocampal and cortical maturation, as indicated for the visual and somatosensory cortices (Cheetham and Fox, 2010). Another possible explanation for these regional differences is that the increased A_1R activation in the hippocampus with maturation dampens the probability of glutamate release such that insufficient glutamate is released and it fails to activate preNMDARs; yet in conjunction with glutamate released by astrocytes it reaches a level capable of activating the presynaptic mGluRs required for t-LTP but not preNMDARs. Here, we describe a similar mechanism at L4–L2/3 synapses, whereby presynaptic A_1R activation dampens glutamate release, although the amount released together with the glutamate released by astrocytes is still capable of activating mGluRs and probably, preNMDARs. However, more experiments are clearly necessary to clarify the events underlying these changes. In the hippocampus, presynaptic mGluR5 is required for presynaptic t-LTP (Falcón-Moya et al., 2020), where these receptors modulate glutamate release (Rodríguez-Moreno et al., 1998) and plasticity (Gómez-Gonzalo et al., 2015). Here, and unlike the hippocampus, we found that postsynaptic mGlu1R is likely to be necessary for the presynaptically expressed t-LTP found at S1 L4–L2/3 synapses. A maturation-associated shift from the involvement of NMDARs to mGluRs in plasticity was previously found in the hippocampus (Falcón-Moya et al., 2020). Although the same was not found here at cortical S1 L4–L2/3 synapses, where NMDARs mGluRs are involved in LTP.

What is clear from our results is that we have detected a new form of presynaptic LTP, expanding the existence of presynaptic forms of LTP to the somatosensory cortex. Forms of preLTP that are dependent on NMDARs have been described in the hippocampus (McGuinness et al., 2010) and at entorhinal cortex to DG synapses (Min et al., 1998; Jourdain et al., 2007; Pérez-Otaño and Rodríguez-Moreno, 2019; Savtchouk et al., 2019), and preLTP forms independent of NMDARs have also been described at hippocampal mossy fiber (MF)-CA3 synapses (Nicoll and Schmitz, 2005), as well as in the cerebellum (Salin et al., 1996), thalamus (Castro-Alamancos and Calcagnotto, 1999), subiculum (Behr et al., 2009), amygdala (López de Armentia and Sah, 2007), and neocortex (Chen et al., 2009). Although mGluRs were thought to be required for some forms of preLTP in the hippocampus (Perea and Araque, 2007; Gómez-Gonzalo et al., 2015), such preLTP was not induced using STDP protocols.

The somatosensory t-LTP requires postsynaptic calcium and NO

As with other forms of LTP, including t-LTP in the hippocampus, t-LTP requires a rise in Ca^{2+} in the postsynaptic cell and the release of Ca^{2+} from intracellular stores (Castillo, 2012; Padamsey and Emptage, 2014; Padamsey et al., 2017; Falcón-Moya et al., 2020; Mateos-Aparicio and Rodríguez-Moreno, 2020). These features of cortical t-LTP are also common to other forms of preLTP (Matyash et al., 2001; Navarrete et al., 2014), and postsynaptic mGluRs are known to recruit postsynaptic calcium stores. We found NO to be the retrograde signal produced by the postsynaptic neuron via Ca^{2+} increase as in other types of preLTP (Castillo, 2012; Padamsey and Emptage, 2014; Padamsey et al., 2017; Falcón-Moya et al., 2020; Mateos-Aparicio and Rodríguez-Moreno, 2020). t-LTP was prevented with aCPTIO but not when L-NAME was loaded into astrocytes. Hence, we concluded that the NO that

participates in this form of t-LTP is not synthetized by astrocytes but rather is released by the postsynaptic neuron and it seems to enter astrocytes to stimulate or modulate the release of gliotransmitters.

Presynaptic t-LTP requires astrocyte signaling

Through two different approaches we demonstrated the involvement of astrocytes in presynaptic t-LTP. First, introducing BAPTA into astrocytes completely prevented t-LTP induction. Second, vesicular release is impaired in dn-SNARE mice, and t-LTP is not observed in slices from these animals. Astrocytes have previously been shown to participate in synaptic potentiation (Jourdain et al., 2007; Perea and Araque, 2007; Savtchouk et al., 2019), yet not as the result of a switch from preLTD to preLTP as we show here at S1 L4–L2/3 synapses. We found that enhanced inhibition of presynaptic release as a result of adenosine activating presynaptic A_1Rs is responsible for the switch from t-LTD to t-LTP during the sixth week of development. Interestingly, A_1R activation at P13–27 converts t-LTD into t-LTP, confirming the importance of adenosine and presynaptic A_1Rs in the switch in plasticity observed, as also found recently in the hippocampus (Falcón-Moya et al., 2020). As found in the hippocampus (Falcón-Moya et al., 2020), our data suggest that adenosine is probably of astrocytic origin. However, as indicated for the loss of t-LTD, although astrocytes clearly participate in this event by probably releasing adenosine, there may also be other sources of this nucleoside (Manzoni et al., 1994). The increase in extracellular adenosine as the barrel cortex matures might be because of increased numbers of astrocytes or to enhanced release, which remains to be defined. As indicated, it may be possible to control plasticity by manipulating the availability of adenosine (Chun et al., 2013; Blundon et al., 2017), and thus adenosine might be an interesting target to improve health, learning, and memory.

Interestingly, and similar to what was found in the hippocampus, adenosine is not the only gliotransmitter necessary for the induction of t-LTP, with ATP/adenosine and glutamate required to mediate t-LTP induction. It is already known that individual astrocytes may release both adenosine and glutamate (Covelo and Araque, 2018), and in this way astrocytes may control basal synaptic activity (Panatier et al., 2011; Falcón-Moya et al., 2020) and tonically depress neurotransmission (Pascual et al., 2005), probably depressing some synapses and potentiating others (Covelo and Araque, 2018). In addition, it is possible that glutamate from the presynaptic neuron also activates preNMDARs but that this amount of glutamate or NMDAR activation is insufficient to drive t-LTP and that glutamate released from astrocytes is also required for t-LTP. It will be interesting to explore what the exact role of the postsynaptic neuron is in the induction of t-LTP and the role of mGluR1. As for the hippocampus, more research is needed to address this question, but surprisingly NO synthesized by the postsynaptic neuron seems to be released and enter the astrocyte, possibly stimulating gliotransmitter release by enhancing the calcium flux into the astrocyte (Matyash, 2001).

At present, it remains unclear what the physiological role of these progressive changes is in plasticity during development that seem to be mainly controlled by the amount of adenosine released by astrocytes at different stages of maturation. Indeed, further studies will be necessary to determine the true influence of STDP in the barrel cortex and the specific developmental role of t-LTD and t-LTP in these circuits. As discussed previously (Pérez-Rodríguez et al., 2019; Falcón-Moya et al., 2020), t-LTD most probably participates in refining synapses, potentially weakening excitatory synapses that are underused or behaviorally irrelevant (Buonomano and Merzenich, 1998; Feldman and Brecht, 2005). The form of presynaptic t-LTP described here is present from the sixth week of development, indicating its relevance from early adulthood onward, when it probably influences learning and memory or other cognitive processes. Presynaptic plasticity may also involve structural changes and may change the short-term properties of neurotransmitter release, participating in circuit computations and changing the excitatory/inhibitory balance or sensory adaptations (Monday et al., 2018). Why some synapses, like L4–L2/3 synapses (and as observed in the hippocampus), show presynaptic and/or postsynaptic plasticity requires further study. Interestingly, STDP of L4–L2/3 and L2/3–L2/3 synapses in the somatosensory cortex has different requirements, indicating that the presynaptic or postsynaptic expression of plasticity is fundamental for the correct functioning of brain circuits and that it is possible they are regulated differently (Banerjee et al., 2009, 2014). Also, and as indicated by some computational models (Costa et al., 2017), presynaptically expressed t-LTP may increase the trial-to-trial reliability, and along with the postsynaptically expressed t-LTP, it may induce a larger change in signal-to-noise ratio than postsynaptic changes alone, as described in auditory cortex (Froemke et al., 2013). In addition, different sites of expression may be an advantage to the system as it may offer more possibilities for plasticity when one is disrupted.

Finally, it may be possible to associate particular behaviors with a particular locus of plasticity. The potential behavioral influence of presynaptic LTP is still an emerging issue for which the data available come from hippocampal MF-CA3 synapses, where preLTP is implicated in learning and memory (Hagena and Manahan-Vaughan, 2011), and from amygdala synapses, where preLTP is implicated in fear memory formation (Tovote et al., 2015). At L4–L2/3 synapses, the behavioral role of presynaptic t-LTP essentially remains to be determined. In the hippocampus, it has been suggested that at CA3–CA1 synapses, preLTP might be associated with learning and memory *in vivo* (Choi et al., 2018). Thus, determining how astrocytes control windows of plasticity by modulating the release of adenosine and other gliotransmitters to refine synapses *in vivo*, and learning and memory, will be of particular interest in the near future. For the moment, from the results described here, it is clear that astrocyte physiology determines, and may significantly affect, the time course of plasticity during development, and as such, in may be possible to open and close windows of plasticity in the somatosensory cortex through pharmacological manipulations.

References

Agmon A, Connors BW (1991) Thalamocortical responses of mouse somatosensory (barrel) cortex in vitro. Neuroscience 41:365–379.

Andrade-Talavera Y, Duque-Feria P, Paulsen O, Rodríguez-Moreno A (2016) Presynaptic spike timing-dependent long-term depression in the mouse hippocampus. Cereb Cortex 26:3637–3654.

Anwyl R (2009) Metabotropic glutamate receptor-dependent long-term potentiation. Neuropharmacology 56:735–740.

Arai A, Kessler M, Lynch G (1990) The effects of adenosine on the development of long-term potentiation. Neurosci Lett 119:41–44.

Araque A, Carmignoto G, Haydon PG, Oliet SH, Robitaille R, Volterra A (2014) Gliotransmitters travel in time and space. Neuron 81:728–739.

Banerjee A, Meredith RM, Rodríguez-Moreno A, Mierau SB, Auberson YP, Paulsen O (2009) Double dissociation of spike timing-dependent potentiation and depression by subunit-preferring NMDA receptors antagonists in mouse barrel cortex. Cereb Cortex 19:2959–2969.

Banerjee A, González-Rueda A, Sampaio-Baptista C, Paulsen O, Rodríguez-Moreno A (2014) Distinct mechanisms of spike timing-dependent LTD at vertical and horizontal inputs onto L2/3 pyramidal neurons in mouse barrel cortex. Physiol Rep 2:e00271.

Banks MI, Hardie JB, Pearce RA (2002) Development of GABA(A) receptor-mediated inhibitory postsynaptic currents in hippocampus. J Neurophysiol 88:3097–3107.

Bear MF, Abraham WC (1996) Long-term depression in hippocampus. Annu Rev Neurosci 19:437–462.

Behr J, Wozny C, Fidzinski P, Schmitz D (2009) Synaptic plasticity in the subiculum. Prog Neurobiol 89:334–342.

Bender VA, Bender KJ, Brasier DJ, Feldman DE (2006) Two coincidence detectors for spike timing-dependent plasticity in somatosensory cortex. J Neurosci 26:4166–4177.

Bi GQ, Poo MM (1998) Synaptic modifications in cultured hippocampal neurons: dependence on spike timing, synaptic strength, and postsynaptic cell type. J Neurosci 18:10464–10472.

Bliss TV, Collingridge GL, Morris RG (2014) Synaptic plasticity in health and disease: introduction and overview. Philos Trans R Soc Lond B Biol Sci 369:20130129.

Blundon JA, Roy NC, Teubner BJW, Yu J, Eom TY, Sample KJ, Pani A, Smeyne RJ, Han SB, Kerekes RA, Rose DC, Hackett TA, Vuppala PK, Freeman BB 3rd, Zakharenko SS (2017) Restoring auditory cortex plasticity in adult mice by restricting thalamic adenosine signaling. Science 356:1352–1356.

Bouvier G, Larsen RS, Rodríguez-Moreno A, Paulsen O, Sjöström PJ (2018) Towards resolving the pressynaptic NMDA receptor debate. Curr Opin Neurobiol 51:1–7.

Brasier DJ, Feldman DE (2008) Synapse-specific expression of functional presynaptic NMDA receptors in rat somatosensory cortex. J Neurosci 28:2199–2211.

Brock JA, Thomazeau A, Watanabe A, Li SSY, Sjöström PJA (2020) A practical guide to using CV analysis for determining the locus of synaptic plasticity. Front Synaptic Neurosci 12:11.

Brzosko Z, Mierau SB, Paulsen O (2019) Neuromodulation of spike-timing-dependent plasticity: past, present and future. Neuron 103:563–581.

Buonomano DV, Merzenich MM (1998) Cortical plasticity: from synapses to maps. Annu Rev Neurosci 21:149–186.

Carter BC, Jahr CE (2016) Postsynaptic, not presynaptic NMDA receptors are required for spike-timing-dependent LTD induction. Nat Neurosci 19:1218–1224.

Castillo PE (2012) Presynaptic LTP and LTD of excitatory and inhibitory synapses. Cold Spring Harb Perspect Biol 4:a005728–a005728.

Castro-Alamancos MA, Calcagnotto ME (1999) Presynaptic long-term potentiation in corticothalamic synapses. J Neurosci 19:9090–9097.

Cheetham CEJ, Fox K (2010) Presynaptic development at L4 to L2/3 excitatory synapses follows different time courses in visual and somatosensory cortex. J Neurosci 30:12566–12571.

Chen HX, Jiang M, Akakin D, Roper SN (2009) Long-term potentiation of excitatory synapses on neocortical somatostatin-expressing interneurons. J Neurophysiol 102:3251–3259.

Choi JH, Sim SE, Kim JI, Choi DI, Oh J, Ye S, Lee J, Kim T, Ko HG, Lim CS, Kaang BK (2018) Interregional synaptic maps among engram cells underlie memory formation. Science 360:430–435.

Chun S, Bayazitov IT, Blundon JA, Zakharenko SS (2013) Thalamocortical long-term potentiation becomes gated after the early critical period in the auditory cortex. J Neurosci 33:7345–7357.

Citri A, Malenka RC (2008) Synaptic plasticity: multiple forms, functions, and mechanisms. Neuropsychopharmacology 33:18–41.

Corlew R, Wang Y, Ghermazien H, Erisir A, Philpot BD (2007) Developmental switch in the contribution of presynaptic and postsynaptic NMDA receptors to long-term depression. J Neurosci 27:9835–9845.

Corlew R, Brasier DJ, Feldman DE, Philpot BD (2008) Presynaptic NMDA receptors: newly appreciated roles in cortical synaptic function and plasticity. Neuroscientist 14:609–625.

Costa RP, Mizusaki BE, Sjöstrom PJ, van Rossum MC (2017) Functional consequences of pre- and postsynaptic expression of synaptic plasticity. Phil Trans R Soc B 372:20160153.

Covelo A, Araque A (2018) Neuronal activity determines distinct gliotransmitter release from a single astrocyte. Elife 7:e32237.

de Mendonça A, Ribeiro JA (1994) Endogenous adenosine modulates long-term potentiation in the hippocampus. Neuroscience 62:385–390.

Debanne D, Gähwiler BH, Thompson SM (1994) Asynchronous pre- and postsynaptic activity induces associative long-term depression in area CA1 of the rat hippocampus in vitro. Proc Natl Acad Sci U S A 91:1148–1152.

Debanne D, Gahwiler BH, Thompson SM (1998) Long-term synaptic plasticity between pairs of individual CA3 pyramidal cells in rat hippocampal slice cultures. J Physiol 507:237–247.

Dunwiddie TV, Masino SA (2001) The role and regulation of adenosine in the central nervous system. Annu Rev Neurosci 24:31–55.

Falcón-Moya R, Pérez-Rodríguez M, Prius-Mengual J, Andrade-Talavera Y, Arroyo-García LE, Pérez-Artés R, Mateos-Aparicio P, Guerra-Gomes S, Oliveira JF, Flores G, Rodríguez-Moreno A (2020) Astrocyte-mediated switch in spike timing-dependent plasticity during hippocampal development. Nat Commun 11:4388.

Feldman DE (2000) Timing-based LTP and LTD at vertical inputs to layer II/III pyramidal cells in rat barrel cortex. Neuron 27:45–56.

Feldman DE (2012) Spike timing-dependence of plasticity. Neuron 75:556–571.

Feldman DE, Brecht M (2005) Map plasticity in somatosensory cortex. Science 310:810–815.

Froemke RC, Carcea I, Barker AJ, Yuan K, Seybold BA, Martins ARO, Zaika N, Bernstein H, Wachs M, Levis PA, Polley DB, Merzenich MM, Schreiner CE (2013) Long-term modification of cortical synapses improves sensory perception. Nat Neurosci 16:79–88.

Gómez-Gonzalo M, Navarrete M, Perea G, Covelo A, Martin-Fernández M, Shigemoto R, Luján R, Araque A (2015) Endocannabinoids induce lateral long-term potentiation of transmitter release by stimulation of gliotransmission. Cereb Cortex 25:3699–3712.

González-Rueda A, Pedrosa V, Feord RC, Clopath C, Paulsen O (2018) Activity-dependent downscaling of subthreshold synaptic inputs during slow-wave-sleep like activity in vivo. Neuron 97:1244–1252.

Hagena H, Manahan-Vaughan D (2011) Learning-facilitated synaptic plasticity at CA3 mossy fiber and commissural-associational synapses reveals different roles in information processing. Cereb Cortex 21:2442–2449.

Hensch TK (2004) Critical period regulation. Annu Rev Neurosci 27:549–579.

Hensch TK (2005) Critical period plasticity in local cortical circuits. Nat Rev Neurosci 6:877–888.

Huckstepp RT, id Bihi R, Eason R, Spyer KM, Dicke N, Willecke K, Marina N, Gourine AV, Dale N (2010) Connexin hemichannel-mediated CO_2-dependent release of ATP in the medulla oblongata contributes to central respiratory chemosensitivity. J Physiol 588:3901–3920.

Inglebert Y, Aljadeff J, Brunel N, Debanne D (2020) Synaptic plasticity rules with physiological calcium levels. Proc Natl Acad Sci U S A 117:33639–33648.

Jo YH, Schlichter R (1999) Synaptic corelease of ATP and GABA in cultured spinal neurons. Nat Neurosci 2:241–245.

Jourdain P, Bergersen LH, Bhaukaurally K, Bezzi P, Santello M, Domercq M, Matute C, Tonello F, Gundersen U, Volterra A (2007) Glutamate exocytosis from astrocytes controls synaptic strength. Nat Neurosci 10:331–339.

Kerr M, Wall MJ, Richardson MJE (2013) Adenosine A_1 receptor activation mediates the developmental shift at layer 5 pyramidal cell synapses and is determinant of mature synaptic strength. J Physiol 591:3371–3380.

Klyuch BP, Dale N, Wall MJ (2012) Deletion of ecto-5′-nucleotidase (CD73) reveals direct action potential-dependent adenosine release. J Neurosci 32:3842–3847.

López de Armentia M, Sah P (2007) Bidirectional synaptic plasticity at nociceptive afferents in the rat central amygdala. J Physiol 581:961–970.

Lovatt D, Xu Q, Liu W, Takano T, Smith NA, Schnermann J, Tieu K, Nedergaard M (2012) Neuronal adenosine release and not astrocytic ATP release mediates feedback inhibition of excitatory activity. Proc Natl Acad Sci U S A 109:6265–6270.

Manzoni OJ, Manabe T, Nicoll RA (1994) Release of adenosine by activation of NMDA receptors in the hippocampus. Science 265:2098–20101.

Markram H, Lübke J, Frotscher M, Sakmann B (1997) Regulation of synaptic efficacy by coincidence of postsynaptic APs and EPSPs. Science 275:213–215.

Mateos-Aparicio P, Rodríguez-Moreno A (2020) Calcium dynamics and synaptic plasticity. Adv Exp Med Biol 1131:965–984.

Matyash V, Filippov V, Mohrhagen K, Kettenmann H (2001) Nitric oxide signals parallel fiber activity to Bergmann glial cells in the mouse cerebellar slice. Mol Cell Neurosci 18:664–670.

McGuinness L, Taylor C, Taylor RD, Yau C, Langenhan T, Hart M, Christian H, Tynan P, Donnelly P, Emptage N (2010) Presynaptic NMDARs in the hippocampus facilitate transmitter release at theta frequency. Neuron 68:1109–1127.

Mederos S, González-Arias C, Perea G (2018) Astrocyte-neuron networks: a multilane highway of signaling for homeostatic brain function. Front Synaptic Neurosci 10:45.

Meredith RM, Floyer-Lea AM, Paulsen O (2003) Maturation of long-term potentiation induction rules in rodent hippocampus: role of GABAergic inhibition. J Neurosci 23:11142–11146.

Min MY, Asztely F, Kokaia M, Kullmann DM (1998) Long-term potentiation and dual component quantal signaling in the dentate gyrus. Proc Natl Acad Sci U S A 95:4702–4707.

Min R, Nevian T (2012) Astrocyte signaling controls spike timing-dependent depression at neocortical synapses. Nat Neurosci 15:746–753.

Monday HR, Younts TJ, Castillo PE (2018) Long-term plasticity of neurotransmitter release: emerging mechanisms and contributions to brain function and disease. Annu Rev Neurosci 41:299–322.

Navarrete M, Díez A, Araque A (2014) Astrocytes in endocannabinoid signalling. Philos Trans R Soc Lond B Biol Sci 369:20130599.

Nevian T, Sakmann B (2006) Spine Ca^{2+} signaling in spike-timing-dependent plasticity. J Neurosci 26:11001–11013.

Nicoll RA, Schmitz D (2005) Synaptic plasticity at hippocampal mossy fibre synapses. Nat Rev Neurosci 6:863–876.

Padamsey Z, Emptage N (2014) Two sides to long-term potentiation: a view towards reconciliation. Philos Trans R Soc Lond B Biol Sci 369:20130154.

Padamsey Z, Tong R, Emptage N (2017) Glutamate is required for depression but not potentiation of long-term presynaptic function. Elife 6:e29688.

Panatier A, Vallée J, Haber M, Murai KK, Lacaille JC, Robitaille R (2011) Astrocytes are endogenous regulators of basal transmission at central synapses. Cell 146:785–798.

Parpura V, Zorec R (2010) Gliotransmission: exocytotic release from astrocytes. Brain Res Rev 63:83–92.

Pascual O, Casper KB, Kubera C, Zhang J, Revilla-Sanchez R, Sul JY, Takano H, Moss SJ, McCarthy K, Haydon PG (2005) Astrocytic purinergic signaling coordinates synaptic networks. Science 310:113–116.

Paulsen O, Moser EI (1998) A model of hippocampal memory encoding and retrieval: GABAergic control of synaptic plasticity. Trends Neurosci 21:273–278.

Perea G, Araque A (2007) Astrocytes potentiate transmitter release at single hippocampal synapses. Science 317:1083–1086.

Pérez-Otaño I, Rodríguez-Moreno A (2019) Presynaptic NMDARs and astrocytes ally to control circuit-specific information flow. Proc Natl Acad Sci U S A 116:13166–13168.

Pérez-Rodríguez M, Arroyo-García LE, Prius-Mengual J, Andrade-Talavera Y, Armengol JA, Pérez-Villegas EM, Duque-Feria P, Flores G, Rodríguez-Moreno A (2019) Adenosine receptor-mediated developmental loss of spike timing-dependent depression in the hippocampus. Cereb Cortex 29:3266–3281.

Pigott M, Garthwaite J (2016) Nitric oxide is required for l-type Ca(2+) channel-dependent long-term potentiation in the hippocampus. Front Synaptic Neurosci 8:17.

Ramón y Cajal S (1894) The Croonian lecture: la fine structure des centres nerveux. Proc Royal Soc London 55:444–468.

Rex CS, Kramár EA, Colgin LL, Lin B, Gall CM, Lynch G (2005) Long-term potentiation is impaired in middle-aged rats: regional specificity and reversal by adenosine receptor antagonists. J Neurosci 25:5956–5966.

Ribot J, Breton R, Calvo CF, Moulard J, Ezan P, Zapata J, Samama K, Moreau M, Bemelmans AP, Sabatet V, Dingli F, Loew D, Milleret C, Billuart P, Dallérac G, Rouach N (2021) Astrocytes close the mouse critical period for visual plasticity. Science 373:77–81.

Rodríguez-Moreno A, Paulsen O (2008) Spike timing-dependent long-term depression requires presynaptic NMDA receptors. Nat Neurosci 11:744–745.

Rodríguez-Moreno A, Sistiaga A, Lerma J, Sánchez-Prieto J (1998) Switch from facilitation to inhibition of excitatory synaptic transmission by group I mGluR desensitization. Neuron 21:1477–1486.

Rodríguez-Moreno A, Banerjee A, Paulsen O (2010) Presynaptic NMDA receptors and spike timing-dependent depression at cortical synapses. Front Synaptic Neurosci 2:18.

Rodríguez-Moreno A, Kohl MM, Reeve J, Eaton TR, Collins HA, Anderson HL, Paulsen O (2011) Presynaptic induction and expression of timing-dependent long-term depression demonstrated by compartment specific photorelease of a use-dependent NMDA antagonist. J Neurosci 31:8564–8569.

Rodríguez-Moreno A, González-Rueda A, Banerjee A, Upton ML, Craig M, Paulsen O (2013) Presynaptic self-depression at developing neocortical synapses. Neuron 77:35–42.

Salin PA, Malenka RC, Nicoll RA (1996) Cyclic AMP mediates a presynaptic form of LTP at cerebellar parallel fiber synapses. Neuron 16:797–803.

Sardinha VM, Guerra-Gomes S, Caetano I, Tavares G, Martins M, Reis JS, Correia JS, Teixeira-Castro A, Pinto L, Sousa N, Oliveira JF (2017) Astrocytic signaling supports hippocampal-prefrontal theta synchronization and cognitive function. Glia 65:1944–1960.

Savtchouk I, Di Castro MA, Ali R, Stubbe H, Luján R, Volterra A (2019) Circuit-specific control of the medial entorhinal inputs to the dentate gyrus by atypical presynaptic NMDARs activated by astrocytes. Proc Natl Acad Sci U S A 116:13602–13610.

Sebastião AM, Cunha RA, de Mendonça A, Ribeiro JA (2000) Modification of adenosine modulation of synaptic transmission in the hippocampus of aged rats. Br J Pharmacol 131:1629–1634.

Sultan S, Li L, Moss J, Petrelli F, Cassé F, Gebara E, Lopatar J, Pfrieger FW, Bezzi P, Bischofberger J, Toni N (2015) Synaptic integration of adult-born hippocampal neurons is locally controlled by astrocytes. Neuron 88:957–972.

Tovote P, Fadok JP, Lüthi A (2015) Neuronal circuits for fear and anxiety. Nat Rev Neurosci 16:317–331.

Wall MJ, Dale N (2013) Neuronal transporter and astrocytic ATP exocytosis underlie activity-dependent adenosine release in the hippocampus. J Physiol 591:3853–3871.

zur Nedden S, Hawley S, Pentland N, Hardie DG, Doney AS, Frenguelli BG (2011) Intracellular ATP influences synaptic plasticity in area CA1 of rat hippocampus via metabolism to adenosine and activity-dependent activation of A1 receptors. J Neurosci 31:6221–6234.